63-3-4

MECHANICAL TECHNOLOGY INCORPORATED

MTI-63TR15

STABILITY ANALYSIS OF GAS LUBRICATED SELF-ACTING PLAIN CYLINDRICAL BEARINGS OF FINITE LENGTH, USING GALERKIN'S METHOD

By

H.S. Cheng
C.H.T. Pan

TECHNICAL REPORT

No. MTI-63TR15
Date April 19, 1963

STABILITY ANALYSIS OF GAS LUBRICATED SELF-ACTING PLAIN CYLINDRICAL JOURNAL BEARINGS OF FINITE LENGTH, USING GALERKIN'S METHOD

By

H.S. Cheng
C.H.T. Pan

H.S. Cheng C.H.T. Pan
Author(s)

Ben Sternlicht
Approved by

H. Gokarian
Approved by

Prepared under

Contract Nonr 3730(00)(FBM)

Supported by

OFFICE OF NAVAL RESEARCH
Department of the Navy

Administered by

OFFICE OF NAVAL RESEARCH
Department of the Navy

MECHANICAL TECHNOLOGY INCORPORATED
LATHAM, N.Y.

MTI-23 (1-63)

TABLE OF CONTENTS

ABSTRACT

The present paper extends the method of Cheng and Trumpler [5] to study stability of plain cylindrical gas journal bearings of finite length. Both equilibrium and stability results have been obtained.

INTRODUCTION

It has been shown recently by many authors, [1 - 10] that one of the most important considerations in designing a high speed gas-lubricated self-acting journal bearing is the instability of the journal under a given operating condition. Intensive research in this direction has led to a number of significant contributions in the past five years.

The first attempt on this stability problem was accomplished by Sternlicht and Rentzepis[2]. Their analysis includes only partial effect of the time variation of pressure in the Reynolds equation. The results predicted, for the first time, the existance of the worst clearance ratio at which the threshold speed of instability is minimum. The same results also indicate the stability is enhanced by a large compressibility number.

Recently Castelli and Elrod[6], Ausman[8], and Cheng and Trumpler[5] have provided stability solutions for the infinitely long bearing. The results of these investigations show reasonably close agreement.

A detailed summary and comparison of experimental data and various solutions to this problem are included in a recent work by Pan and Sternlicht[16]. They also give the results of a stability analysis using the quasi-static linearized ph stability solution of the Reynolds equation for bearings of finite length.

The major obstacle in this problem lies in the difficulty to obtain an accurate solution of the non-linear Reynolds equation with the time dependent term. The method of B. G. Galerkin applied to the function ph [5] has proven to be a very effective way to handle equations of this kind. It has the main advantage of reducing the Reynolds equation directly from the partial differential equation to a system of first order ordinary differential equations which together with the equations of motion of the journal yield quite readily to stability analysis of the system. It also can be applied to bearings of more complicated configurations such as partial arc bearings, so long as a dependable quantitative description of the ph function can be guessed.

The present report is essentially the extension of the work[5] to the stability study of finite journal bearings using Galerkin's method.

I. GOVERNING EQUATIONS

Considering a finite length journal and bearing system as shown in Fig. 1, the equation governing the pressure in the gas film is the isothermal Reynolds equation.

$$\frac{\partial}{\partial \xi}\left(PH^3 \frac{\partial P}{\partial \xi}\right) + \frac{\partial}{\partial \theta}\left(PH^3 \frac{\partial P}{\partial \theta}\right) = \Lambda \left(1 - 2\dot{\alpha}\right) \frac{\partial (PH)}{\partial \theta} + 2\,\frac{\partial (PH)}{\partial \tau} \quad \ldots\ldots\ldots\ldots \quad (1)$$

where

$$P = \frac{p}{p_a}$$

$$H = 1 + \epsilon \cos \theta$$

$$\epsilon = \frac{e}{C}$$

$$\xi = \frac{z}{R}$$

$$\Lambda = \frac{6\mu\omega}{p_a} \left(\frac{R}{C}\right)^2$$

$$\dot{\alpha} = \frac{d\alpha}{d\tau}$$

$$\tau = \omega t$$

Assuming the journal is perfectly balanced and that it rotates at a constant rotational speed, the equations governing the translational motion (as opposed to the conical motion) of the journal become

$$\frac{1}{2\pi} \int_{-\frac{L}{D}}^{+\frac{L}{D}} \delta\, d\xi \int_0^{2\pi} P \cos\theta\, d\theta + P_m \cos\alpha - \frac{MC\omega^2}{p_a L D}\left(\ddot{\epsilon} - \epsilon \dot{\alpha}^2\right) = 0 \qquad (2)$$

$$\frac{1}{2\pi} \int_{-\frac{L}{D}}^{+\frac{L}{D}} \delta\, d\xi \int_0^{2\pi} P \sin\theta\, d\theta - P_m \sin\alpha - \frac{MC\omega^2}{p_a L D}\left(\epsilon \ddot{\alpha} + 2\dot{\alpha}\dot{\epsilon}\right) = 0 \qquad (3)$$

where

$$\delta = \frac{\pi}{2}\frac{D}{L}$$

$$P_m = \frac{F}{p_a L D}$$

Let ψ = PH, equation (1) becomes

$$\frac{\partial}{\partial \xi}\left(H\psi\frac{\partial \psi}{\partial \xi}\right) + \frac{\partial}{\partial \theta}\left[\psi\left(H\frac{\partial \psi}{\partial \theta} - \psi\frac{\partial H}{\partial \theta}\right)\right] = \Lambda\left[(1-2\dot{\alpha})\frac{\partial \psi}{\partial \theta} + 2\frac{\partial \psi}{\partial \tau}\right] \quad \ldots\ldots\ldots\ldots\ (4)$$

In order to apply the method of Galerkin to equation (4), we assume

$$\psi = H + \sum_{n=1}^{N} \sum_{m=1}^{M} \Big[C_n \cos(2n-1)\bar{\xi} + A_{nm} \cos m\theta \cos(2n-1)\bar{\xi}$$

$$+ B_{nm} \sin m\theta \cos(2n-1)\bar{\xi}\Big] \quad \ldots\ldots\ldots\ (5)$$

where $\bar{\xi} = \frac{\pi}{2}\frac{D}{L}\xi$

Using Galerkin's method for m = 2 and n = 1, equations (2), (3) and (4) are reduced to

$$\left[K_6 C_1 + K_3 A_{11} + (K_6 - K_8) A_{12}\right] + P_m \cos\alpha - \frac{Mc\omega^2}{P_a L D}\left(\ddot{\epsilon} - \epsilon\dot{\alpha}^2\right) = 0 \quad \ldots\ldots\ldots\ (6)$$

$$\left[K_5 B_{11} + K_8 B_{12}\right] - P_m \sin\alpha - \frac{Mc\omega^2}{P_a L D}\left(\epsilon\ddot{\alpha} + 2\dot{\alpha}\dot{\epsilon}\right) = 0 \quad \ldots\ldots\ldots\ (7)$$

$$2\Lambda\frac{dc_1}{d\tau} + \delta^2\left(1 + \frac{\epsilon^2}{2}\right) C_1 + \delta^2\epsilon A_{11} + \frac{4\delta^2 C_1^2}{3\pi} + \frac{\delta^2\epsilon^2}{4} A_{12}$$

$$+ \frac{2\delta^2}{3\pi}\left(A_{11}^2 + B_{11}^2 + A_{12}^2 + B_{12}^2\right) + \frac{2\delta^2}{3\pi}\epsilon\left(A_{11}A_{12} + B_{11}B_{12}\right)$$

$$+ \frac{4\delta^2}{3\pi}\epsilon C_1 A_{11} = 0 \quad \ldots\ldots\ldots\ (8)$$

$$2\Lambda \frac{dA_{11}}{d\tau} + \frac{8}{\pi}\Lambda \frac{d\epsilon}{d\tau} + 2\Lambda B_{11}\left(\frac{1}{2} - \dot{\alpha}\right) + \Big[(1+\delta^2) A_{11} + (2\delta^2 - 1)\, \epsilon C_1$$

$$+ (2\delta^2 + 5)\frac{\epsilon A_{12}}{2} + \frac{8}{3\pi}(1+\delta^2)\, C_1 A_{11} + \frac{3}{4}\epsilon^2 \delta^2 A_{11} + \frac{4}{3\pi}(\delta^2 - 2)\, \epsilon C_1^2$$

$$+ \frac{4}{3\pi}(4+\delta^2)\, \epsilon A_{12} C_1 + \frac{4}{3\pi}(1+\delta^2)(A_{11}A_{12} + B_{11}B_{12}) + \frac{(4+\delta^2)}{3\pi}\epsilon (A_{11}^2 - B_{11}^2)$$

$$+ \frac{2}{3\pi}(\delta^2 - 2)\, \epsilon \,(A_{11}^2 + A_{12}^2 + B_{11}^2 + B_{12}^2) \Big] = 0 \quad \ldots\ldots\ldots\ldots\ldots\ldots\ldots \quad (9)$$

$$2\Lambda \frac{dA_{12}}{d\tau} + 2\Lambda (1 - 2\dot{\alpha}) B_{12} + \Big[(\delta^2 - 2)\frac{\epsilon^2}{2} C_1 + (\delta^2 + 1)\, \epsilon A_{11}$$

$$+ \frac{\epsilon^2}{2}(4+\delta^2) A_{12} + \frac{8}{3\pi}(4+\delta^2)\, C_1 A_{12} + \frac{4}{3\pi}(\delta^2 - 2)\, \epsilon C_1 A_{11}$$

$$+ \frac{2}{3\pi}(4+\delta^2)(A_{11}^2 - B_{11}^2) + \frac{4}{3\pi}(4+\delta^2)\, \epsilon A_{11} A_{12} - \frac{8}{\pi}\epsilon B_{11} B_{12} = 0 \quad \ldots\ldots \quad (10)$$

$$2\Lambda \frac{dB_{11}}{d\tau} - \frac{4\Lambda}{\pi}(1 - 2\dot{\alpha})\epsilon - 2\Lambda\left(\frac{1}{2} - \dot{\alpha}\right) A_{11} + \Big[(1+\delta^2) B_{11}$$

$$+ \frac{(5 + 2\delta^2)}{2}\epsilon B_{12} + \frac{(4+\delta^2)}{4}\epsilon^2 B_{11} + \frac{8}{3\pi}(1+\delta^2)\, C_1 B_{11}$$

$$+ \frac{4}{3\pi}(4+\delta^2)\, \epsilon B_{12} C_1 + \frac{4(1+\delta^2)}{3\pi}(A_{11}B_{12} - A_{12}B_{11}) + \frac{2}{3\pi}(4+\delta^2)\, \epsilon A_{11} B_{11} = 0 \quad \ldots \quad (11)$$

$$2\Lambda \frac{dB_{12}}{d\tau} - 2\Lambda(1-2\dot{\alpha})A_{12} + \Big[(4+\delta^2)B_{12} + \frac{\epsilon^2}{2}(4+\delta^2)B_{12}$$

$$+ (\delta^2+1)\epsilon B_{11} + \frac{8}{3\pi}(4+\delta^2)C_1B_{12} + \frac{4}{3\pi}(\delta^2-2)\epsilon C_1B_{11}$$

$$+ \frac{4}{3\pi}(4+\delta^2)A_{11}B_{11} + \frac{4}{3\pi}(4+\delta^2)\epsilon A_{11}B_{12} + \frac{8}{\pi}\epsilon A_{11}B_{11}\Big] = 0 \qquad (12)$$

The detail derivations of equations (6) to (12) are included in Appendix I.

III. EQUILIBRIUM SOLUTION

By setting all derivatives equal to zero in equations (6) through (12), we obtain readily the equations governing the static equilibrium position of the journal. Numerical solutions of equation (8) through (12) for $C_{1o}, A_{11o}, B_{11o}, B_{12o}$ can be obtained, using Newton-Raphson's method [17]. Once C_{1o}, A_{11o} etc. are determined, the expression for the load and attitude angle can be derived from eqs. (6) and (7). They are

$$P_m = \frac{1}{\pi}\left\{\left[K_{6o}C_{1o} + K_{3o}A_{11o} + (K_{6o} - K_{8o})A_{12o}\right]^2 + \left[K_{5o}B_{11o} + K_{8o}B_{12o}\right]^2\right\}^{1/2} \quad \ldots\ldots\ldots (13)$$

$$\tan \alpha_o = -\frac{K_{5o}B_{11o} + K_{8o}B_{12o}}{K_{6o}C_{1o} + K_{3o}A_{11o} + (K_{6o} - K_{8o})A_{12o}} \quad \ldots\ldots\ldots\ldots\ldots (14)$$

The results of the equilibrium solution are tabulated in Tables 1 to 4 and plotted as the load and attitude angle charts in Figs. 2 to 9. Comparison between the present solution with two finite difference numerical solutions [11], [12] is also shown in Figs. 10 to 13.

In general, the present results compare quite favorably with finite difference computer results. The largest error introduced by using Galerkin's approximation appears to fall in two regions:

1. High ϵ and low Λ region:- In this region, the present theory predicts a lower load and a higher attitude angle than finite difference solutions. This type of error is due to the truncation error of the assumed function in the θ direction. The same characteristic error was also observed in the analysis of infinitely long bearings.
2. Large $\frac{L}{D}$ and high Λ region:- In this region, the Galerkin method gives a slightly lower load and attitude angle comparing to finite difference solutions. The reason for this error is that only one cosine term is assumed in the axial direction. It is

conceivable that the results will be much improved if more terms are considered in the axial direction. However, the algebraic complexity introduced by assuming more terms in the axial direction would also become much more formidable.

IV. STABILITY OF THE EQUILIBRIUM SOLUTION

The stability of the equilibrium solution can be investigated by considering a small perturbed displacement of the journal center and small variations of the pressure coefficients, C, A, etc., which are defined by

$$\begin{aligned}
\epsilon &= \epsilon_o + \epsilon^* \\
\alpha &= \alpha_o + \alpha^* \\
C_1 &= C_o + C_1^* \\
A_{11} &= A_{11o} + A_{11}^* \\
A_{12} &= A_{12o} + A_{12}^* \\
B_{11} &= B_{11o} + B_{11}^* \\
B_{12} &= B_{12o} + B_{12}^*
\end{aligned} \qquad \dots\dots\dots\dots \quad (15)$$

Substituting (15) into equations (6) to (12), and neglecting all non-linear terms, we obtain the linearized equations of the dynamical system which can be written in the matrix form as

$$AX + I\,\frac{dX}{d\tau} = 0 \qquad \dots\dots\dots\dots \quad (16)$$

where the column matrix X represents

$$X = \begin{vmatrix} \dot{\alpha}^* \\ \alpha^* \\ \dot{\epsilon}^* \\ \epsilon \\ C^* \\ A_{11}^* \\ B_{11}^* \\ A_{12}^* \\ B_{12}^* \end{vmatrix} \qquad \dots\dots\dots\dots \quad (17)$$

I is the unit matrix and A is a 9 x 9 coefficient matrix whose elements are expressed in terms of the parameters P_m, Λ, $\frac{L}{D}$, and equilibrium solutions ϵ_o, γ_o, C_{1o},A_{11o} etc. A complete list of these coefficients is given in Appendix II.

The characteristic equation for the system represented by equation (16) is a nineth degree polynomial whose coefficients can be determined numerically by using Danielewsky's method [15] . After the characteristic equation is determined, the stability of the equilibrium solution can be investigated by applying Routh's Criterion [14] to the coefficients of the polynomial. For a given set of parameters $\frac{L}{D}$, ϵ_o, and Λ, it is found that there exists a threshold speed below which the journal position is stable and above which, unstable. The numerical calculation of the polynomial coefficients as well as the threshold speeds are performed on an IBM 7090 digital computer. The results of the threshold speed for different values of $\frac{L}{D}$, ϵ_o and Λ are tabulated in tables 1 to 4 and also are plotted as the stability charts in Figs. 14 to 17.

The whirl frequency of the system at the threshold of stability can be determined by extracting the roots of the characteristic polynomial at the threshold speed. The complex conjugate roots which have a nearly zero real part are identified as the whirl frequency, since its real part is at the threshold of becoming positive. Complete whirl frequency maps are calculated for $\frac{L}{D}$ equal to 1 and 1/4 and are shown in Figs. 18 and 19.

The parameters used in the analysis are convenient for computation. They cannot be directly used for design purpose, since both the parameters $\omega\left(\frac{MC}{F}\right)^{1/2}$ and Λ involve the rotational speed. Another set of stability parameters more suitable for designing purpose was first given by Rentzepis and Sternlicht. The advantage of that plot is that the speed can be varied independently without changing other parameters. The conversion of the present stability data to $\bar{C}$ and $\bar{\omega}$ plot are shown in Fig 20 and 21 for $\frac{L}{D} = 2$ and 1/2.

V. DISCUSSION OF RESULTS

1. Equilibrium Solutions

The overall agreement between the equilibrium solutions by the Galerkin method and the finite difference method is quite encouraging, considering the assumed functions for ph only include a few leading terms of the Fourier series. The error contributed by the insufficient terms in the circumferential direction becomes more pronounced for small $\frac{L}{D}$, large ϵ and small Λ. The error of load factor for $\frac{L}{D} = 1/2$, $\epsilon = 0.8$ varies from 1% to 10% in the high Λ region and rises to approximately 35% in the low Λ region. The error disappears rapidly with decreasing ϵ. The second type of error is attributed to the insufficient terms in the axial direction. Since only a single cosine term is chosen in this axial direction, it is expected that the error will be amplified when both $\frac{L}{D}$ and Λ become large, regardless of the value of ϵ. For $\frac{L}{D} = 2$, $\epsilon = 0.1$, $\Lambda = 100$, this type of error increases to 18% for the load factor.

2. Stability Curves

In general, the stability curves show the same trend as those obtained earlier for the infinitely long bearing. Plotting the threshold speeds for small values of Λ (on regular-scale graph paper), one can show that the threshold speed tends to approach zero as Λ goes to zero, regardless of the value of ϵ and $\frac{L}{D}$. This fact verifies the theory that a non-cavitated full film incompressible journal bearing is unstable.

For constant values of $\frac{L}{D}$ and ϵ, the stability curve rises rapidly with increasing Λ, forms a hump in the middle range of Λ and finally approaches an asymptote for extremely high Λ. The location of the hump and the maximum threshold speed depend greatly on $\frac{L}{D}$ and ϵ. However, the asymptotic speed at high Λ for each ϵ seems to change little with different values of $\frac{L}{D}$.

For $\frac{L}{D}$ equal to 1/2 and 1/4, ϵ equal to 0.8 and 0.9, and high values of Λ, the present theory fails to predict a meaningful threshold speed. In this region, Routh's Criterion gives a very low threshold speed with

the corresponding whirl frequency many times higher than 1/2. It is extremely difficult to determine whether this low threshold speed actually exists in reality or is caused by an extraneous root due to the truncation error in the assumed function. This region represents either extremely heavily loaded or low ambient cases and thus is of little practical interest. Such uncertain results in this region are discarded.

3. Whirl Frequency Curves

The whirl frequency curves show that for a fixed $\frac{L}{D}$ and ϵ, the frequency approaches an asymptote at small Λ, reaches a minimum value in the middle range of Λ and finally approaches half-frequency at extremely high Λ. It should be of interest to compare the asymptotic frequency at small Λ with that of an incompressible experiment.

4. Comparison with an Earlier Theory

The comparison of the present stability curves and Pan and Sternlicht's Quasi-Static theory [16] shows general agreement in trend for large values of Λ (see Figs. 22, 23). On the $\bar{C}$ and $\bar{\omega}$ plot, they seem to give similar slopes for a constant P_m, but the present theory predicts a higher threshold speed in this region. At small Λ region, the two theories give quite different slopes with the present theory predicting a more conservative threshold speed.

5. Comparison with Experiment

Unfortunately, there exist only a few experimental data for comparison. Fig. 22 shows some comparison with results made by Sternlicht and Winn [9], and Whitley-Bowhill-McEwan [7]. For $\frac{L}{D} = 1$ and $P_m =$ 0.2, agreement is excellent in small Λ region, but less satisfactory in high Λ region. For $\frac{L}{D} = 2$ and $P_m = 0.1$, agreement is very good with Sternlicht-Winn's upper curve (the upper curve is the spontaneous instability, while the lower data is obtained by giving an impulsive force at successive speeds, and the speed at which the stability cannot be restored is considered as the threshold speed). It is surprising that the

few data obtained by Whitley-Bowhill and McEwan fall extremely close to the present stability curves. Such close agreement is probably accidental.

The comparison with Reynolds and Gross [10] data is shown in Fig. 23. These curves seem to show a consistent trend, that the agreement is very close at Λ values smaller than 1, but less satisfactory in higher Λ region.

VI. CONCLUSIONS

1. The method of Galerkin provides an effective technique to solve the time-dependent non-linear Reynolds equation, and it lends itself very conveniently in determining the stability curves for various operating parameters.

2. The stability results using Galerkin's method show the same trend indicated by earlier work (see Fig. 22). For example, a minimum threshold speed is shown to exist in all theories when varying the clearance under constant load. Also, the effect of $\frac{L}{D}$ is similar as given by Pan and Sternlicht.

3. Comparison of the present stability results with available experimental data is encouraging (see Figs. 23, 24).

VII. RECOMMENDATIONS

1. More experimental data is needed to establish a consistent correlation with theoretical results such as given in this paper.

2. The non-linear Galerkin method should be applied to analyze the partial arc bearings to obtain both equilibrium and stability results. (This analysis is presently under way at MTI.)

3. The response of the cylindrical gas journal under finite dynamic load (particularly impulsive load) can be studied by performing time-wise integration of the simultaneous, ordinary differential equations on either an analog or digital computer.

4. The present analysis can be readily extended to consider the stability problem for the conical mode of a symmetrical rotor bearing system. It also can be extended to study the dynamics of a non-symmetrical rotor. (This analysis is presently under way at MTI.)

APPENDIX I

Derivation of eq. (8) to eq. (12)

Substituting eq. (15) into the left side of eq. (4), we have

$$\frac{\partial}{\partial \xi}\left(H\psi\frac{\partial \psi}{\partial \xi}\right)+\frac{\partial}{\partial \theta}\left[\psi\left(H\frac{\partial \psi}{\partial \theta}-\psi\frac{\partial H}{\partial \theta}\right)\right] =$$

$$\sum_{m=1}^{N} C_n\left[\epsilon(\cos\theta+\epsilon\cos 2\theta)-(1+\epsilon\cos\theta)^2(2n-1)^2\delta^2\right]\cos(2n-1)\xi$$

$$-\sum_{m=1}^{M}\sum_{n=1}^{N}\left\{A_{nm}\left[\frac{\epsilon^2}{4}(m+1)(m-2)\cos(m-2)\theta+\epsilon\left(m+\frac{1}{2}\right)(m-1)\cos(m-1)\theta\right.\right.$$
$$+\left(1+\frac{\epsilon^2}{2}\right)m^2\cos m\theta+\epsilon\left(m-\frac{1}{2}\right)(m+1)\cos(m+1)\theta+\frac{\epsilon^2}{4}(m-1)(m+2)\cos(m+2)\theta$$
$$\left.+(2n-1)^2\delta^2(1+\epsilon\cos\theta)^2\cos m\theta\right]+B_{nm}\left[\frac{\epsilon^2}{4}(m+1)(m-2)\sin(m-2)\theta\right.$$
$$+\epsilon\left(m+\frac{1}{2}\right)(m-1)\sin(m-1)\theta+\left(1+\frac{\epsilon^2}{2}\right)m^2\sin m\theta+\epsilon\left(m-\frac{1}{2}\right)(m+1)\sin(m+1)\theta$$
$$\left.\left.+\frac{\epsilon^2}{4}(m-1)(m+2)\sin(m+2)\theta+(2n-1)^2\delta^2(1+\epsilon\cos\theta)^2\sin m\theta\right]\right\}\cos(2n-1)\xi$$

$$+\sum_{\ell=1}^{N}\sum_{n=1}^{N}C_\ell C_n\left\{\frac{\epsilon}{2}\cos\theta\left[\cos 2(\ell+n-1)\xi+\cos 2(\ell-n)\xi\right]-(2n-1)\delta^2(1+\epsilon\cos\theta)\right.$$
$$\left.\left[(\ell+n-1)\cos 2(\ell+n-1)\xi+(\ell-n)\cos 2(\ell-n)\xi\right]\right\}$$

$$-\sum_{\ell=1}^{N}\sum_{m=1}^{M}\sum_{n=1}^{N}C_\ell A_{nm}\left\{\frac{1}{2}\left[m^2\cos m\theta+\frac{\epsilon}{2}(m+1)(m-1)\cos(m+1)\theta+\frac{\epsilon}{2}(m+1)(m-1)\cos(m-1)\theta\right]\right.$$
$$\left[\cos 2(\ell+n-1)\xi+\cos 2(\ell-n)\xi\right]+(2n-1)\delta^2(1+\epsilon\cos\theta)\cos m\theta$$
$$\left.\left[(\ell+n-1)\cos 2(\ell+n-1)\xi+(\ell-n)\cos 2(\ell-n)\xi\right]\right\}$$

$$-\sum_{\ell=1}^{N}\sum_{m=1}^{M}\sum_{n=1}^{N}C_\ell B_{nm}\left\{\frac{1}{2}\left[m^2\sin m\theta+\frac{\epsilon}{2}(m+1)(m-1)\sin(m+1)\theta+\frac{\epsilon}{2}(m+1)(m-1)\sin(m-1)\theta\right]\right.$$
$$\left[\cos 2(\ell+n-1)\xi+\cos 2(\ell-n)\xi\right]+(2n-1)\delta^2(1+\epsilon\cos\theta)\sin m\theta$$
$$\left.\left[(\ell+n-1)\cos 2(\ell+n-1)\xi+(\ell-n)\cos 2(\ell-n)\xi\right]\right\}$$

$$
\begin{aligned}
&+\sum_{k=1}^{M}\sum_{l=1}^{N}\sum_{n=1}^{N} A_{lk}C_n\Big\{\frac{\epsilon}{4}\big[(k+1)\cos(k+1)\theta-(k-1)\cos(k-1)\theta\big]\big[\cos 2(l+n-1)\bar{\xi}+\cos 2(l-n)\bar{\xi}\big]\\
&\qquad -(2n-1)\delta^2(1+\epsilon\cos\theta)\cos k\theta\big[(l+n-1)\cos 2(l+n-1)\bar{\xi}+(l-n)\cos 2(l-n)\bar{\xi}\big]\Big\}
\end{aligned}
$$

$$
\begin{aligned}
&+\sum_{k=1}^{M}\sum_{l=1}^{N}\sum_{n=1}^{N} B_{lk}C_n\Big\{\frac{\epsilon}{4}\big[(k+1)\sin(k+1)\theta-(k-1)\sin(k-1)\theta\big]\big[\cos 2(l+n-1)\bar{\xi}+\cos 2(l-n)\bar{\xi}\big]\\
&\qquad -(2n-1)\delta^2(1+\epsilon\cos\theta)\sin k\theta\big[(l+n-1)\cos 2(l+n-1)\bar{\xi}+(l-n)\cos 2(l-n)\bar{\xi}\big]\Big\}
\end{aligned}
$$

$$
\begin{aligned}
&-\sum_{k=1}^{M}\sum_{l=1}^{N}\sum_{m=1}^{M}\sum_{n=1}^{N} A_{lk}A_{nm}\Big\{\frac{1}{4}\big[m(m+k)\cos(m+k)\theta+m(m-k)\cos(m-k)\theta\\
&\qquad +\frac{\epsilon}{2}(m-1)(m+k+1)\cos(m+k+1)\theta+\frac{\epsilon}{2}(m-1)(m-k+1)\cos(m-k+1)\theta\\
&\qquad +\frac{\epsilon}{2}(m+1)(m+k-1)\cos(m+k-1)\theta+\frac{\epsilon}{2}(m+1)(m-k-1)\cos(m-k-1)\theta\big]\\
&\qquad \big[\cos 2(l+n-1)\bar{\xi}+\cos 2(l-n)\bar{\xi}\big]+(2n-1)\delta^2(1+\epsilon\cos\theta)\cos k\theta\cos m\theta\\
&\qquad \big[(l+n-1)\cos 2(l+n-1)\bar{\xi}+(l-n)\cos 2(l-n)\bar{\xi}\big]\Big\}
\end{aligned}
$$

$$
\begin{aligned}
&-\sum_{k=1}^{M}\sum_{l=1}^{N}\sum_{m=1}^{M}\sum_{n=1}^{N} B_{lk}A_{nm}\Big\{\frac{1}{4}\big[m(m+k)\sin(m+k)\theta-m(m-k)\sin(m-k)\theta\\
&\qquad +\frac{\epsilon}{2}(m-1)(m+k+1)\sin(m+k+1)\theta-\frac{\epsilon}{2}(m-1)(m-k+1)\sin(m-k+1)\theta\\
&\qquad +\frac{\epsilon}{2}(m+1)(m+k-1)\sin(m+k-1)\theta-\frac{\epsilon}{2}(m+1)(m-k-1)\sin(m-k-1)\theta\big]\\
&\qquad \big[\cos 2(l+n-1)\bar{\xi}+\cos 2(l-n)\bar{\xi}\big]+(2n-1)\delta^2(1+\epsilon\cos\theta)\sin k\theta\cos m\theta\\
&\qquad \big[(l+n-1)\cos 2(l+n-1)\bar{\xi}+(l-n)\cos 2(l-n)\bar{\xi}\big]\Big\}
\end{aligned}
$$

$$
\begin{aligned}
&-\sum_{k=1}^{M}\sum_{l=1}^{N}\sum_{m=1}^{M}\sum_{n=1}^{N} A_{lk}B_{nm}\Big\{\frac{1}{4}\big[m(m-k)\sin(m-k)\theta+(m+k)m\sin(m+k)\theta\\
&\qquad +\frac{\epsilon}{2}(m-1)(m-k+1)\sin(m-k+1)\theta+\frac{\epsilon}{2}(m-1)(m+k+1)\sin(m+k+1)\theta\\
&\qquad +\frac{\epsilon}{2}(m+1)(m+k-1)\sin(m+k-1)\theta+\frac{\epsilon}{2}(m+1)(m-k-1)\sin(m-k-1)\theta\big]\\
&\qquad \big[\cos 2(l+n-1)\bar{\xi}+\cos 2(l-n)\bar{\xi}\big]+(2n-1)\delta^2(1+\epsilon\cos\theta)\cos k\theta\sin m\theta\\
&\qquad \big[(l+n-1)\cos 2(l+n-1)\bar{\xi}+(l-n)\cos 2(l-n)\bar{\xi}\big]\Big\}
\end{aligned}
$$

$$- \sum_{k=1}^{M}\sum_{l=1}^{N}\sum_{m=1}^{M}\sum_{n=1}^{N} B_{lk}B_{nm}\Big\{ \frac{1}{4}\Big[m(m+k)\cos(m+k)\theta + m(k-m)\cos(k-m)\theta$$
$$+ \frac{\epsilon}{2}(m-1)(m+k+1)\cos(m+k+1)\theta + \frac{\epsilon}{2}(m-1)(k-m-1)\cos(k-m-1)\theta$$
$$+ \frac{\epsilon}{2}(m+1)(k+m-1)\cos(k+m-1)\theta + \frac{\epsilon}{2}(m+1)(k-m+1)\cos(k-m+1)\theta\Big]$$
$$\Big[\cos 2(l+n-1)\bar{\xi} + \cos 2(l-n)\bar{\xi}\Big] + (2n-1)\delta^{2}(1+\epsilon\cos\theta)\sin k\theta \sin m\theta$$
$$\Big[(l+n-1)\cos 2(l+n-1)\bar{\xi} + (l-n)\cos 2(l-n)\bar{\xi}\Big]\Big\} \qquad (A1)$$

Letting

$$\mathcal{R}(\psi) = \frac{\partial}{\partial\theta}\Big[\psi\Big(H\frac{\partial\psi}{\partial\theta} - \psi\frac{\partial H}{\partial\theta}\Big)\Big] + \frac{\partial}{\partial\xi}\Big(\psi H\frac{\partial\psi}{\partial\xi}\Big) - \Lambda(1-2\dot{\alpha})\frac{\partial\psi}{\partial\theta} - 2\Lambda\frac{\partial\psi}{\partial\xi} \qquad (A2)$$

then the Galerkin procedure gives the following set of equations:

$$\int_{-\frac{\pi}{2}}^{+\frac{\pi}{2}}\int_{0}^{2\pi} \mathcal{R}(\psi)\cos(2r-1)\bar{\xi}\; d\bar{\xi}\, d\theta = 0 \qquad r = 1, \cdots N \qquad (A3)$$

$$\int_{-\frac{\pi}{2}}^{+\frac{\pi}{2}}\int_{0}^{2\pi} \mathcal{R}(\psi)\cos(2r-1)\bar{\xi}\cos p\theta\, d\bar{\xi}\, d\theta = 0 \qquad \begin{matrix} r = 1, \cdots N \\ p = 1, \cdots M \end{matrix} \qquad (A4)$$

$$\int_{-\frac{\pi}{2}}^{+\frac{\pi}{2}}\int_{0}^{2\pi} \mathcal{R}(\psi)\cos(2r-1)\bar{\xi}\sin q\theta\, d\bar{\xi}\, d\theta = 0 \qquad \begin{matrix} r = 1, \cdots N \\ q = 1, \cdots M \end{matrix} \qquad (A5)$$

Substituting (A1) into (A3), (A4), and (A5), and letting M = 2 and N = 1, we have eq. (8) to eq. (12).

Derivation of eq. (6) and eq. (7)

After substituting ψ into the fluid force terms in the equations of motion, the radial force becomes

$$F_r = \frac{1}{2\pi}\int_{-\frac{\pi}{2}}^{+\frac{\pi}{2}}\int_0^{2\pi}\frac{\psi}{H}\cos\theta\, d\theta\, d\xi$$

$$= \frac{1}{2\pi}\int_{-\frac{\pi}{2}}^{+\frac{\pi}{2}}\cos\xi\, d\xi\int_0^{2\pi}\frac{\cos\theta}{H}(H + C_1 + A_{11}\cos\theta + B_{11}\sin\theta + A_{12}\cos 2\theta + B_{12}\sin 2\theta)\, d\theta$$

$$= \frac{1}{\pi}\left[K_6 C_1 + K_3 A_{11} + (K_6 - K_8)A_{12}\right] \qquad (A6)$$

Similarly, the tangential force becomes

$$F_\theta = \frac{1}{2\pi}\int_{-\frac{\pi}{2}}^{+\frac{\pi}{2}}\int_0^{2\pi}\frac{\psi}{H}\sin\theta\, d\theta\, d\xi$$

$$= \frac{1}{2\pi}\int_{-\frac{\pi}{2}}^{+\frac{\pi}{2}}\cos\xi\, d\xi\int_0^{2\pi}\frac{\sin\theta}{H}(H + C_1 + A_{11}\cos\theta + B_{11}\sin\theta + A_{12}\cos 2\theta + B_{12}\sin 2\theta)\, d\theta$$

$$= \frac{1}{\pi}(K_5 B_{11} + K_8 B_{12}) \qquad (A7)$$

where

$$K_3 = \frac{2\pi}{S(S+1)}$$

$$K_5 = \frac{2\pi}{S+1}$$

$$K_6 = -\frac{2\pi\epsilon}{S(S+1)} \qquad (A8)$$

$$K_8 = -\frac{2\pi\epsilon}{(S+1)^2}$$

$$S = (1-\epsilon^2)^{1/2}$$

APPENDIX II

LINEARIZATION

Equations (6) to (12) are linearized by expanding each term in Taylor's series with respect to the equilibrium solution and only keeping the linear term. The procedure is straightforward; therefore, only two examples will be given here and the rest results are listed as the coefficients in table 5.

1. Linearization of F_r

$$\begin{aligned} F_r &= K_6 C_1 + K_3 A_{11} + (K_6 - K_8) A_{12} \\ &\cong K_{60} C_{1_0} + K_{3_0} A_{11_0} + (K_{6_0} - K_{8_0}) A_{12_0} \\ &\quad + \left[\frac{\partial K_6}{\partial \epsilon} C_{1_0} + \frac{\partial K_3}{\partial \epsilon} A_{11_0} + \left(\frac{\partial K_6}{\partial \epsilon} - \frac{\partial K_8}{\partial \epsilon} \right) A_{12_0} \right] \epsilon^* \\ &\quad + K_{6_0} C_1^* + K_{3_0} A_{11}^* + (K_{6_0} - K_{8_0}) A_{12}^* \end{aligned} \tag{A9}$$

2. Linearization of $\frac{2\delta^2}{3\pi} \epsilon (A_{11} A_{12} + B_{11} B_{12})$

$$\begin{aligned} \frac{2\delta^2}{3\pi} \epsilon (A_{11} A_{12} + B_{11} B_{12}) &\cong \frac{2\delta^2}{3\pi} \Big[\epsilon_0 (A_{11_0} A_{12_0} + B_{11_0} B_{12_0}) \\ &\quad + (A_{11_0} A_{12_0} + B_{11_0} B_{12_0}) \epsilon^* + \epsilon_0 (A_{11_0} A_{12}^* + A_{12_0} A_{11}^* + B_{11_0} B_{12}^* + B_{12_0} B_{11}^*) \Big] \end{aligned} \tag{A10}$$

where the subscript o represents the equilibrium solution.

NOMENCLATURE

A	Coefficient matrix of the stability equation.
C_1, $A_{11}, B_{11}, A_{12}, B_{12}$	Pressure coefficients.
C	Radial clearance, in. (also used as a pressure coeff.).
$\bar{C}$	$\left[\left(\frac{MR}{F}\right) \left(\frac{P_a}{6\mu}\right)^2 \right]^{1/5} \frac{C}{R}$ dimensionless clearance.
D	Diameter of the journal, in.
e	Eccentricity, in.
F	Load, lb.
F_r	Radial load, lb.
F_θ	Tangential load, lb.
h	Film thickness, in.
H	Dimensionless film thickness.
I	Unit matrix.
m, n, k, l	Index for the pressure coefficients.
M, N	Index for the order of approximation of ph function.
p, q, r	See equations (A3), (A4) and (A5).
L	Length of the journal, in.
K_3	$\frac{2\pi}{S(S+1)}$
K_5	$\frac{2\pi}{S+1}$
K_6	$-\frac{2\pi\epsilon}{S(S+1)}$

K_8	$-\dfrac{2\pi\epsilon}{(S+1)^2}$
δ	$\dfrac{\pi}{2}\ \dfrac{D}{L}$
M	Mass of the journal, slug.
p	Pressure, psia
p_a	Ambient pressure, psia
P	p/p_a
P_m	$\dfrac{F}{p_a LD}$
R	Radius of the journal, in.
S	$(1 - \epsilon^2)^{1/2}$
t	Time, sec.
X	See definition (17)
z	Coordinate in the axial direction, in.
ϵ	Eccentricity ratio.
μ	Viscosity, lb. sec./in.^{2}
τ	ωt
α	Attitude angle.
θ	Coordinates in the circumferential direction.
ξ	z/R
ω	Rotational speed of the journal.
$\bar{\omega}$	$\left[\left(\dfrac{MR}{R}\right)^2 \left(\dfrac{6\mu}{p_a}\right) \right]^{1/5} \omega$
ψ	PH
Λ	$\dfrac{6\mu\omega}{p_a} \left(\dfrac{R}{C}\right)^2$
λ	$\dfrac{\text{whirl frequency}}{\omega}$
Ω	$\dfrac{Mc\omega^2}{p_a LD}$

REFERENCES

1. Arwas, E.B., Sternlicht, B., Poritsky, H., "Dynamic Stability Aspects of Cylindrical Journal Bearings Using Compressible and Incompressible Fluids", Proceedings of First International Symposium on Gas-Lubricated Bearings, Washington, D.C., 1959.

2. Sternlicht, B., Rentzepis, G.M., "On the Stability of Rotors in Cylindrical Journal Bearings", paper number 61-WA-196, Presented at Winter Meeting of ASME, New York, November 26 - December 1, 1961.

3. Pan, C.H.T., and Sternlicht, B., "On the Translatory Whirl Motion of a Vertical Rotor in Plain Cylindrical Gas-Dynamic Journal Bearings," ASME Transactions, D, March 1962.

4. Pan, C.H.T., "On the Time Dependent Effects of Self-Acting Gas Journal Bearings," Report No. MTI-62TR1, February 1962, Mechanical Technology Incorporated, Latham, New York.

5. Cheng, H.S. and Trumpler, P.R., "Stability of the High Speed Journal Bearing Under Steady Load," presented at the ASME Winter Annual Meeting Nov. 1962, paper No. 62-WA-101.

6. Castelli, V., Elrod, H.G., "Two Approaches to the Solution of the Stability Problem for 360° Gas Lubricated Journal Bearings," Interim Report No. I-A2049-20, The Franklin Institute, Philadelphia, Pa., June 1962.

7. Whitley, S., Bowhill, A.J. and McEwan, P., "The Load Capacity and Half-Speed Whirl of Hydrodynamic Gas Journal Bearings," UKAEA Report DEG 199(CA), 1960.

8. Ausman, J S., "Linearized PH Stability Theory for Translatory Half-Speed Whirl of Long Self-Acting Gas-Lubricated Journal Bearings," presented at Winter Meeting of ASME, New York, New York, November 26 - December 1, 1962.

9. Sternlicht, B. and Winn, L.W., "On The Load Capacity and Stability of Rotors in Cylindrical Gas-Dynamic Journal Bearings," Technical Report under Contract NONR 2844(00) Task Nr. 097-348, General Electric Company, Schenectady, New York, July, 1961.

10. Reynolds, D.B. and Gross, W.A., "Experimental Investigation of Whirl in Self-Acting Air-Lubricated Journal Bearings," Research Report RJ-198 under contract NONR 3448(00) Task Nr. 061-120, International Business Machines Corporation, Research Laboratory, San Jose, California, October 1961.

11. Sternlicht, B., "Gas-Lubricated Cylindrical Journal Bearings of the Finite Length, Static Loading," Journal of Applied Mechanics, ASME Transactions E, December 1961, p. 535.

12. Raimondi, A.A., "A numerical Solution for the Gas-Lubricated Full Journal Bearing of Finite Length," ASLE Paper No. 60-L-C-14.

13. McCann, R.A., "Stability of Unloaded Gas-Lubricated Bearings," presented at the ASME-ASLE Lubrication Conference, Pittsburgh, Pa., Oct. 16-18, 1962.

14. Gantmacher, F.R., "Applications of the Theory of Matrices," (Translated from Russian), first edition, Interscience Publishers, 1959

15. Faddeeva, V.N., "Computational Methods of Linear Algebra," (Translated from Russian), Dover Publications, Inc., New York, p. 166.

16. Pan, C.H.T., and Sternlicht, B , "Comparison Between Theories and Experiments for the Threshold of Instability of Rigid Rotors in Self-Acting Plain Cylindrical Journal Bearings," to be presented at the ASME 1963 Spring Lubrication Symposium, Boston, Mass.

17. Scarborough, J.B., "Numerical Mathematical Analysis," The Johns-Hopkins Press, 1955.

LIST OF TABLES

TABLE 1

Load, Attitude Angle and Threshold Speed for $\frac{L}{D} = 2$

ϵ	Λ	P_m	α_o	$\omega(\frac{MC}{F})^{\frac{1}{2}}$
0.1	0.1	0.00789	86.38	0.3203
	0.5	0.03774	72.50	0.6356
	1.0	0.0672	57.87	0.7846
	2.0	0.0997	38.70	0.8765
	5.0	0.1227	17.83	0.8697
	10.0	0.1275	9.141	0.8221
	20.0	0.1288	4.600	0.7900
	100.0	0.1292	0.922	0.7838
0.2	0.1	0.01596	86.16	0.4453
	0.5	0.07622	71.55	0.9115
	1.0	0.1357	56.69	1.1038
	2.0	0.2033	37.92	1.2331
	5.0	0.2548	17.56	1.2235
	10.0	0.2660	9.011	1.1566
	20.0	0.2691	4.535	1.1114
	100.0	0.2700	0.909	1.1027
0.4	0.1	0.0332	85.23	0.6797
	0.5	0.1593	67.79	1.3647
	1.0	0.2863	52.03	1.6046
	2.0	0.4431	34.72	1.7487
	5.0	0.5916	16.48	1.7419
	10.0	0.6298	8.489	1.6262
	20.0	0.6405	4.275	1.5563
	100.0	0.6440	0.8568	1.5381
0.6	0.1	0.0529	83.61	0.9609
	0.5	0.2620	61.44	1.8993
	1.0	0.4916	44.41	2.0997
	2.0	0.7953	29.10	2.1407
	5.0	1.1491	14.46	2.0988
	10.0	1.2655	7.5402	1.9431
	20.0	1.2997	3.8035	1.8444
	100.0	1.3110	0.7626	1.8084
0.8	0.1	0.0777	80.56	1.4765
	0.5	0.4319	50.84	2.901
	1.0	0.9081	33.01	3.0202
	2.0	1.5684	20.54	2.5896
	5.0	2.4178	10.80	2.3519
	10.0	2.7931	5.805	2.1038
	20.0	2.9146	2.943	1.9641
	100.0	2.955	0.591	1.8950
0.9	0.1	0.0967	76.81	2.0391
	0.5	0.6340	40.76	5.1056
	1.0	1.4938	24.17	4.497
	2.0	2.7078	14.34	2.9075
	5.0	4.2546	7.7261	2.4816
	10.0	5.0487	4.2665	2.1617
	20.0	5.3265	2.1758	1.9844
	100.0	5.4211	0.4373	1.9146

TABLE 2

Load, Attitude Angle and Threshold Speed for $\frac{L}{D} = 1$

ϵ	Λ	P_m	α_o	$\omega(\frac{MC}{F})^{\frac{1}{2}}$	λ
0.1	0.1	0.00370	88.29	.2578	.4976
	0.5	0.01831	81.52	.5559	.4979
	1.0	0.03551	73.43	.7556	.4985
	2.0	0.06394	59.38	.9387	.4996
	5.0	0.10551	34.32	1.0340	.4997
	10.0	0.12180	18.90	.9774	.4996
	20.0	0.12757	9.72	.9240	.4998
	50.0	0.12899	3.92	.9023	.5000
	100.0	0.12914	1.96	.8953	.5000
0.2	0.1	0.00758	88.11	.3671	.4902
	0.5	0.03747	80.68	.7974	.4912
	1.0	0.07249	71.97	1.0778	.4935
	2.0	0.12998	57.48	1.3388	.4979
	5.0	0.21650	33.08	1.4487	.4986
	10.0	0.25291	18.25	1.3751	.4982
	20.0	0.26547	9.39	1.2945	.4992
	50.0	0.26935	3.79	1.2693	.4999
	100.0	0.26992	1.89	1.2593	.5000
0.4	0.1	0.01660	87.34	.5703	.4567
	0.5	0.08201	77.07	1.2386	.4595
	1.0	0.15829	65.86	1.6354	.4667
	2.0	0.28302	49.96	1.9101	.4840
	5.0	0.48529	28.38	2.0071	.4918
	10.0	0.58882	15.85	1.9051	.4917
	20.0	0.62882	8.19	1.7935	.4965
	50.0	0.64164	3.31	1.7304	.4993
	100.0	0.64353	1.65	1.7237	.4998
0.6	0.1	0.02861	85.75	.85156	.3968
	0.5	0.14364	69.90	1.8162	.3978
	1.0	0.28529	54.90	2.3057	.4014
	2.0	0.52462	38.24	2.5309	.4180
	5.0	0.92022	21.43	2.4221	.4536
	10.0	1.16019	12.33	2.2424	.4713
	20.0	1.26773	6.46	2.0759	.4888
	50.0	1.30417	2.62	1.9867	.4980
	100.0	1.30965	1.31	1.9790	.4995
0.8	0.1	0.04635	82.29	1.3671	.3230
	0.5	0.25550	56.43	2.9426	.2984
	1.0	0.56879	38.32	3.7185	.2715
	2.0	1.12187	23.92	3.6096	.2909
	5.0	1.96448	13.13	3.0526	.3498
	10.0	2.52521	7.93	2.4862	.4214
	20.0	2.82464	4.26	2.1657	.4712
	50.0	2.93462	1.74	——	——
	100.0	2.95150	0.87	——	——
0.9	0.1	0.060917	78.12	1.9140	.2867
	0.5	0.39428	44.07	5.2711	.1846

Table 2 (con'td.)

ϵ	Λ	P_m	α_o	$\omega(\frac{MC}{F})^{\frac{1}{2}}$	λ
0.9	1.0	0.98910	26.83	7.2323	.1414
	2.0	2.04802	15.71	4.3436	.2354
	5.0	3.54985	8.41	3.3341	.3091
	10.0	4.55718	5.21	2.6243	.3892
	20.0	5.14859	2.86	——	——
	50.0	5.37737	1.18	——	——
	100.0	5.41302	0.59	——	——

TABLE 3

Load, Attitude Angle and Threshold Speed for $\frac{L}{D} = \frac{1}{2}$

ϵ	Λ	P_m	α_o	$\omega\left(\frac{MC}{F}\right)^{\frac{1}{2}}$
0.1	0.1	0.00119	89.45	0.1484
	0.5	0.00592	87.24	0.3432
	1.0	0.01180	84.50	0.4881
	2.0	0.02329	79.11	0.6787
	5.0	0.05357	64.51	0.9916
	10.0	0.08673	46.67	1.1233
	20.0	0.11302	28.08	1.0794
	100.0	0.12843	6.11	0.9698
0.2	0.1	0.00246	89.37	0.2266
	0.5	0.01227	86.85	0.5027
	1.0	0.02444	83.73	0.7148
	2.0	0.04809	77.68	0.9884
	5.0	0.1095	62.14	1.4131
	10.0	0.1770	44.55	1.5842
	20.0	0.2333	26.79	1.5285
	100.0	0.2682	5.83	1.3553
0.4	0.1	0.00564	89.00	0.3672
	0.5	0.02816	85.03	0.8090
	1.0	0.05600	80.18	1.1440
	2.0	0.10960	71.27	1.5461
	5.0	0.2443	52.42	2.0836
	10.0	0.3930	36.43	2.2220
	20.0	0.5345	22.02	2.0918
	100.0	0.6383	4.84	1.8548
0.6	0.1	0.01050	88.12	0.5859
	0.5	0.05259	80.69	1.2909
	1.0	0.10561	72.03	1.7901
	2.0	0.21172	58.03	2.3845
	5.0	0.48124	36.89	3.0831
	10.0	0.7613	24.83	3.1493
	20.0	1.0468	15.42	2.5649
	100.0	1.2959	3.50	2.0991
0.8	0.1	0.01882	85.69	1.0547
	0.5	0.09810	69.50	2.3483
	1.0	0.21447	53.78	3.3849
	2.0	0.4877	36.00	4.9782
	5.0	1.1580	19.50	3.0627
	10.0	1.7351	12.82	2.2672
	20.0	2.3152	8.315	3.3919
	100.0	2.9150	2.000	—
0.9	0.1	0.02614	82.37	1.5703
	0.5	0.15119	56.42	3.8951
	1.0	0.3809	37.68	9.4715
	2.0	0.9636	22.48	—
	5.0	2.2829	11.35	—
	10.0	3.2816	7.29	—
	20.0	4.2517	4.80	—
	100.0	5.3433	1.20	—

Note: There is no $\Lambda = 50.0$ for L/D = ½

TABLE 4

Load, Attitude Angle and Threshold Speed for $\frac{L}{D} = \frac{1}{4}$

ϵ	Λ	P_m	α_o	$\omega(\frac{MC}{F})^{\frac{1}{2}}$	λ
0.1	.0.1	0.00032	89.85	0.0859	.4995
	0.5	0.00159	89.25	0.1880	.4995
	1.0	0.00319	88.51	0.2643	.4995
	2.0	0.00637	87.01	0.3717	.4996
	5.0	0.01581	82.58	0.5867	.4996
	10.0	0.03087	75.47	0.8158	.4997
	20.0	0.05678	62.84	1.0517	.4999
	50.0	0.09973	38.35	1.1585	.5000
	100.0	0.11944	21.66	1.0770	.4999
0.2	0.1	0.00066	89.82	0.1172	.4971
	0.5	0.00332	89.13	0.2710	.4971
	1.0	0.00665	88.26	0.3811	.4972
	2.0	0.01328	86.52	0.5538	.4972
	5.0	0.03289	81.41	0.8566	.4974
	10.0	0.06379	73.44	1.1712	.4979
	20.0	0.11608	60.22	1.4914	.4991
	50.0	0.20443	36.44	1.6254	.4997
	100.0	0.24769	20.59	1.5047	.4997
0.4	0.1	0.00156	89.71	0.1953	.4759
	0.5	0.00782	88.53	0.4456	.4759
	1.0	0.01563	87.08	0.6335	.4759
	2.0	0.03119	84.19	0.8810	.4760
	5.0	0.07685	75.9	1.3697	.4761
	10.0	0.14691	64.49	1.8244	.4765
	20.0	0.26024	49.58	2.2164	.4780
	50.0	0.46043	29.34	2.2597	.4886
	100.0	0.57632	16.70	2.0567	.4954
0.6	0.1	.00303	89.40	.3203	.4190
	0.5	.01514	87.02	.7357	.4188
	1.0	.03029	84.07	1.0288	.4184
	2.0	.06072	78.33	1.4549	.4160
	5.0	.15282	63.42	2.2107	.4031
	10.0	.29899	47.38	2.8756	.3748
	20.0	.52310	33.06	3.6563	.3237
	50.0	.89971	19.49	3.1921	.3729
	100.0	1.14660	11.41	2.4377	.4603
0.8	0.1	0.00573	88.45	.6328	.3277
	0.5	.02883	82.33	1.4139	.3257
	1.0	.05871	74.98	2.0159	.3188
	2.0	.12455	62.07	2.9215	.2934
	5.0	.37025	38.82	5.6890	.1860
	10.0	.77898	24.54	8.4947	.1283
	20.0	1.30347	15.83	———	———
	50.0	2.0394	9.52	———	———
	100.0	2.5593	5.87	———	———
0.9	0.1	.00820	86.99	1.0078	.2777
	0.5	.04219	75.30	2.2754	.2682

Table 4 (con'td.)

ϵ	Λ	P_m	α_o	$\omega(\frac{MC}{F})^{\frac{1}{2}}$	λ
0.9	1.0	.09099	62.43	3.4042	.2402
	2.0	.22099	44.26	7.0147	.1414
	5.0	.78206	22.95	———	———
	10.0	1.6488	13.63	———	———
	20.0	2.61783	8.49	———	———
	50.0	3.82627	5.07	———	———
	100.0	4.70404	3.22	———	———

TABLE 5

Coefficients for the Linearized Equations (16)

$$a_{11} = 0$$

$$a_{12} = \frac{P_m \cos\alpha_o}{\Omega \; \epsilon_o}$$

$$a_{13} = 0$$

$$a_{14} = \frac{1}{\Omega \epsilon_o} \left[\frac{-2\epsilon_o}{S_o(S_o+1)^2} B_{11o} + \frac{2(2-S_o)}{S_o(S_o+1)^2} B_{12o} \right]$$

$$a_{15} = 0$$

$$a_{16} = 0$$

$$a_{17} = \frac{1}{\Omega \epsilon_o} \left(\frac{-2}{S_o+1} \right)$$

$$a_{18} = 0$$

$$a_{19} = \frac{1}{\Omega} \left[\frac{2}{(S_o+1)^2} \right]$$

$$a_{21} = -1$$

$$a_{22} = a_{23} = a_{24} = a_{25} = a_{26} = a_{27} = a_{28} = a_{29} = 0$$

$$a_{31} = 0$$

$$a_{32} = \frac{P_m}{\Omega} \sin\alpha_o$$

$$a_{33} = 0$$

$$a_{34} = \frac{1}{\Omega} \left[\frac{2(-S_o^2 + S_o + 1)}{S_o^3(S_o+1)} \right] C_{1o} + \left[\frac{-2\epsilon_o(2S_o+1)}{S_o^3(S_o+1)^2} \right] A_{11o} + \left[\frac{2(-2S_o^2+2S_o+1)}{S_o^3(S_o+1)^2} \right] A_{12o}$$

$$a_{35} = \frac{1}{\Omega} \left[\frac{2\epsilon_o}{S_o(S_o+1)} \right]$$

$$a_{36} = \frac{1}{\Omega} \left[\frac{-2}{S_o(S_o+1)} \right]$$

$$a_{37} = 0$$

$$a_{38} = \frac{1}{\Omega}\left[\frac{2\epsilon_0}{S_0(S_0+1)^2}\right]$$

$$a_{39} = 0$$

$$a_{41} = a_{42} = 0$$

$$a_{43} = -1$$

$$a_{44} = a_{45} = a_{46} = a_{47} = a_{48} = a_{49} = 0$$

$$a_{51} = a_{52} = a_{53} = 0$$

$$a_{54} = \frac{\delta^2}{2\Lambda}\left[\epsilon_0 C_{10} + A_{110} + \frac{\epsilon_0}{2}A_{120} + \frac{4}{3\pi}C_{10}A_{110} + \frac{2}{3\pi}\left(A_{110}A_{120} + B_{110}B_{120}\right)\right]$$

$$a_{55} = \frac{\delta^2}{2\Lambda}\left[\left(1 + \frac{\epsilon_0^2}{2}\right) + \frac{8}{3\pi}C_{10} + \frac{4}{3\pi}\epsilon_0 A_{110}\right]$$

$$a_{56} = \frac{\delta^2}{2\Lambda}\left[\epsilon_0 + \frac{4}{3\pi}A_{110} + \frac{4}{3\pi}\epsilon_0 C_{10} + \frac{2}{3\pi}\epsilon_0 A_{120}\right]$$

$$a_{57} = \frac{\delta^2}{2\Lambda}\left[\frac{4}{3\pi}B_{110} + \frac{2}{3\pi}\epsilon_0 B_{120}\right]$$

$$a_{58} = \frac{\delta^2}{2\Lambda}\left[\frac{4}{3\pi}A_{120} + \frac{\epsilon_0^2}{4} + \frac{2}{3\pi}\epsilon_0 A_{110}\right]$$

$$a_{59} = \frac{\delta^2}{2\Lambda}\left[\frac{4}{3\pi}B_{120} + \frac{2}{3\pi}\epsilon_0 B_{110}\right]$$

$$a_{61} = -B_{110}$$

$$a_{62} = 0$$

$$a_{63} = \frac{4}{\pi}$$

$$a_{64} = \left[(2\delta^2-1)C_{10} + \left(\delta^2+\frac{5}{2}\right)A_{120} + \frac{3}{2}\delta^2\epsilon_0 A_{110} + \frac{4}{3\pi}(\delta^2-2)C_{10}^2 + \frac{4}{3\pi}(\delta^2+4)A_{120}C_{10}\right.$$
$$\left. + \frac{\delta^2+4}{3\pi}\left(A_{110}^2 - B_{110}^2\right) + \frac{2}{3\pi}(\delta^2-2)\left(A_{110}^2 + B_{110}^2 + A_{120}^2 + B_{120}^2\right)\right]\frac{1}{2\Lambda}$$

$$a_{65} = \frac{1}{2\Lambda}\left[(2\delta^2-1)\epsilon_0 + \frac{8(\delta^2+1)}{3\pi}A_{110} + \frac{8}{3\pi}(\delta^2-2)\epsilon_0 C_{10} + \frac{4}{3\pi}(\delta^2+4)\epsilon_0 A_{120}\right]$$

$$a_{66} = \frac{1}{2\Lambda}\left[(\delta^2+1) + \frac{3}{4}\epsilon_0^2\delta^2 + \frac{4}{3\pi}(\delta^2+1)A_{120} + \frac{2}{\pi}\delta^2\epsilon_0 A_{120} + \frac{8}{3\pi}(\delta^2+1)C_{10}\right]$$

$$a_{67} = \frac{1}{2} + \frac{1}{2\Lambda}\left[\frac{4}{3\pi}(\delta^2+1)B_{120} + \frac{2}{3\pi}(\delta^2-8)\epsilon_0 B_{120}\right]$$

$$a_{68} = \frac{1}{2\Lambda}\left[(\frac{5}{2}+\delta^2)\epsilon_0 + \frac{4}{3\pi}(\delta^2+4)\epsilon_0 C_{10} + \frac{4}{3\pi}(\delta^2+1)A_{110} + \frac{4}{3\pi}(\delta^2-2)\epsilon_0 A_{120}\right]$$

$$a_{69} = \frac{1}{2\Lambda}\left[\frac{4}{3\pi}(\delta^2+1)B_{110} + \frac{4}{3\pi}(\delta^2-2)\epsilon_0 B_{120}\right]$$

$$a_{71} = A_{110} + \frac{4}{\pi}\epsilon_0$$

$$a_{72} = a_{73} = 0$$

$$a_{74} = \frac{1}{2\Lambda}\left[(\delta^2+\frac{5}{2})B_{120} + \frac{\delta^2+4}{2}\epsilon_0 B_{110} + \frac{4}{3\pi}(\delta^2+4)C_{10}B_{120} + \frac{2}{3\pi}(\delta^2+4)A_{110}B_{110}\right] - \frac{2}{\pi}$$

$$a_{75} = \frac{1}{2\Lambda}\left[\frac{8}{3\pi}(\delta^2+1)B_{110} + \frac{4}{3\pi}(\delta^2+4)\epsilon_0 B_{120}\right]$$

$$a_{76} = -\frac{1}{2} + \frac{1}{2\Lambda}\left[\frac{4}{3\pi}(\delta^2+1)B_{120} + \frac{2}{3\pi}(\delta^2+4)\epsilon_0 B_{110}\right]$$

$$a_{77} = \frac{1}{2\Lambda}\left[(\delta^2+1) + \frac{\delta^2+4}{4}\epsilon_0^2 + \frac{8}{3\pi}(\delta^2+1)C_0 - \frac{4}{3\pi}(\delta^2+1)A_{120} + \frac{2}{3\pi}(\delta^2+4)\epsilon_0 A_{110}\right]$$

$$a_{78} = \frac{1}{2\Lambda}\left[-\frac{4}{3\pi}(\delta^2+1)B_{110}\right]$$

$$a_{79} = \frac{1}{2\Lambda}\left[(\delta^2+\frac{5}{2})\epsilon_0 + \frac{4}{3\pi}(\delta^2+4)\epsilon_0 C_{10} + \frac{4}{3\pi}(\delta^2+1)A_{110}\right]$$

$$a_{81} = -2B_{120}$$

$$a_{82} = a_{83} = 0$$

$$a_{84} = \frac{1}{2\Lambda}\left[(\delta^2-2)\epsilon_0 C_{10} + (\delta^2+1)A_{110} + (\delta^2+4)\epsilon_0 A_{120} + \frac{4}{3\pi}(\delta^2-2)C_0 A_{110}\right.$$
$$\left. + \frac{4}{3\pi}(\delta^2+4)A_{110}A_{120} - \frac{8}{\pi}B_{110}B_{120}\right]$$

$$a_{85} = \frac{1}{2\Lambda}\left[(\delta^2-2)\frac{\epsilon_0^2}{2} + \frac{8}{3\pi}(\delta^2+4)A_{120} - \frac{4}{3\pi}(\delta^2-2)\epsilon_0 A_{110}\right]$$

$$a_{86} = \frac{1}{2\Lambda}\left[(\delta^2+1)\epsilon_0 + \frac{4}{3\pi}(\delta^2-2)\epsilon_0 C_{10} + \frac{4}{3\pi}(\delta^2+4)A_{110} - \frac{4}{3\pi}(\delta^2+4)\epsilon_0 A_{120}\right]$$

$$a_{87} = \frac{1}{2\lambda}\left[-\frac{4}{3\pi}(\delta^2+4)B_{110} - \frac{8}{\pi}\epsilon_o B_{120}\right]$$

$$a_{88} = \frac{1}{2\lambda}\left[\frac{8}{3\pi}(\delta^2+4)C_{10} + \frac{4}{3\pi}(\delta^2+4)\epsilon_o A_{110} + (\delta^2+4)(1+\frac{\epsilon_o^2}{2})\right]$$

$$a_{89} = 1 - \frac{1}{2\lambda}\left(\frac{8}{\pi}\epsilon_o B_{110}\right)$$

$$a_{91} = 2A_{120}$$

$$a_{92} = a_{93} = 0$$

$$a_{94} = \frac{1}{2\lambda}\left[(\delta^2+4)\epsilon_o B_{120} + (\delta^2+1)B_{110} + \frac{4}{3\pi}(\delta^2-2)C_{10}B_{110} + \frac{4}{3\pi}(\delta^2+4)A_{110}B_{120} + \frac{8}{\pi}A_{120}B_{110}\right]$$

$$a_{95} = \frac{1}{2\lambda}\left[\frac{8}{3\pi}(\delta^2+4)B_{120} + \frac{4}{3\pi}(\delta^2-2)\epsilon_o B_{110}\right]$$

$$a_{96} = \frac{1}{2\lambda}\left[\frac{4}{3\pi}(\delta^2+4)B_{110} + \frac{4}{3\pi}(\delta^2+4)\epsilon_o B_{120}\right]$$

$$a_{97} = \frac{1}{2\lambda}\left[(\delta^2+1)\epsilon_o + \frac{4}{3\pi}(\delta^2-2)\epsilon_o C_{10} + \frac{4}{3\pi}(\delta^2+4)A_{110} + \frac{8}{\pi}\epsilon_o A_{120}\right]$$

$$a_{98} = -1 + \frac{1}{2\lambda}\left(\frac{8}{\pi}\epsilon_o B_{110}\right)$$

$$a_{99} = \frac{1}{2\lambda}\left[(\delta^2+4)(1+\frac{\epsilon_o^2}{2}) + \frac{8}{3\pi}(\delta^2+4)C_{10} + \frac{4}{3\pi}(\delta^2+4)\epsilon_o A_{110}\right]$$

LIST OF FIGURES

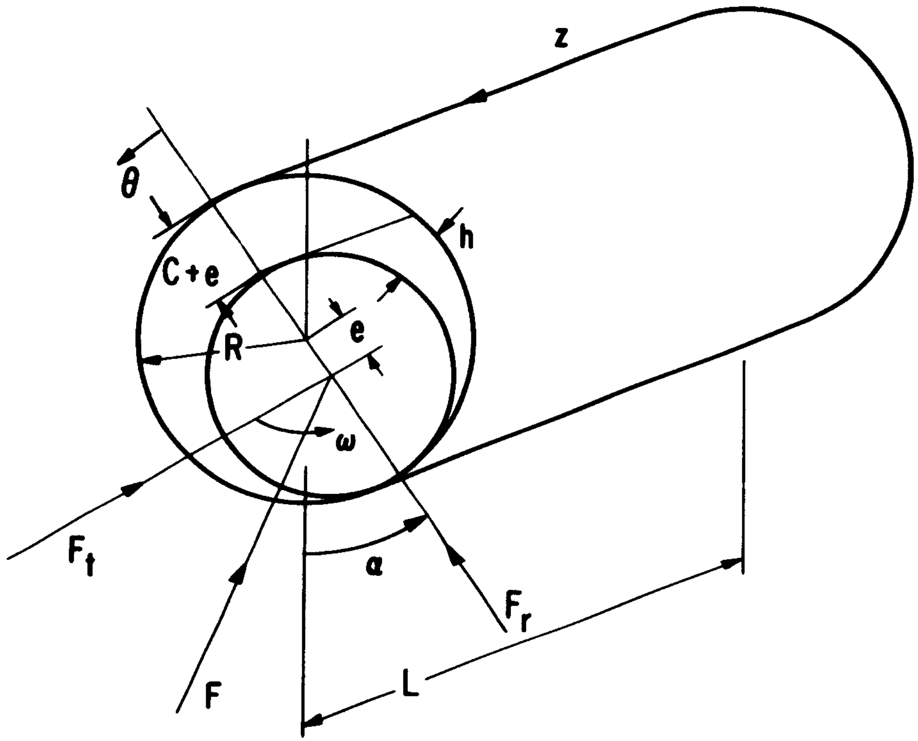

Figure 1. Schematic of a Journal Bearing

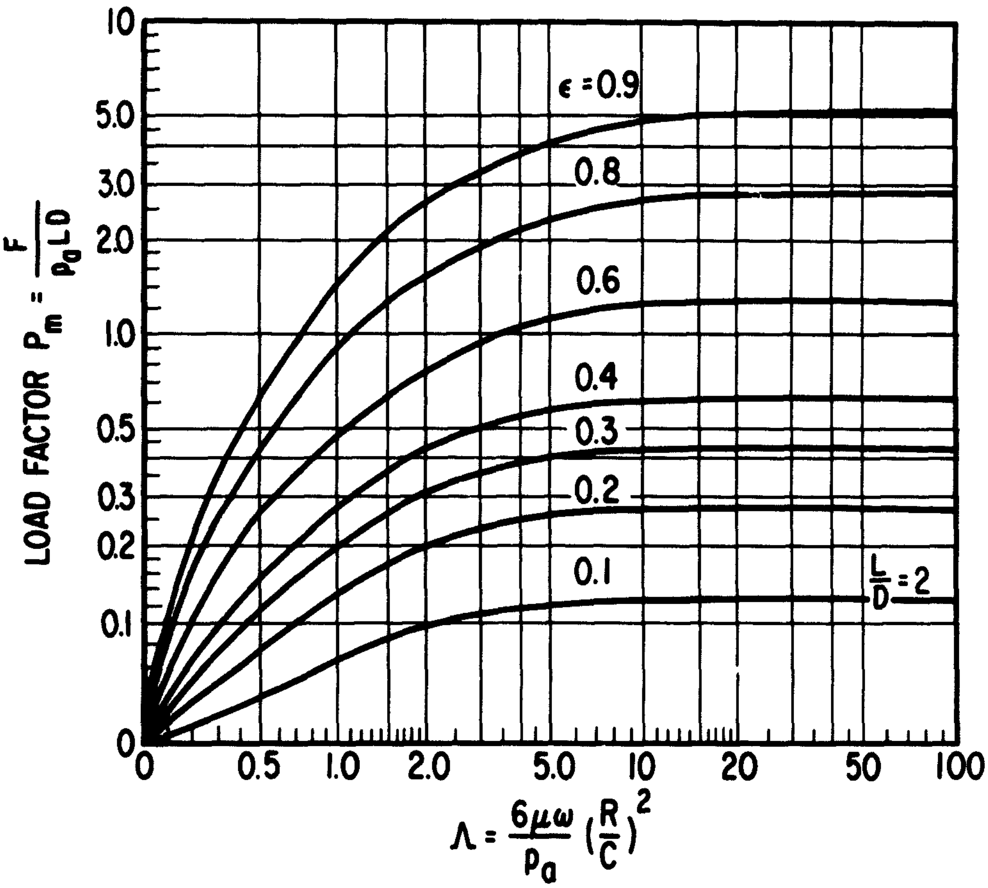

Figure 2 Load Chart for $\frac{L}{D} = 2$

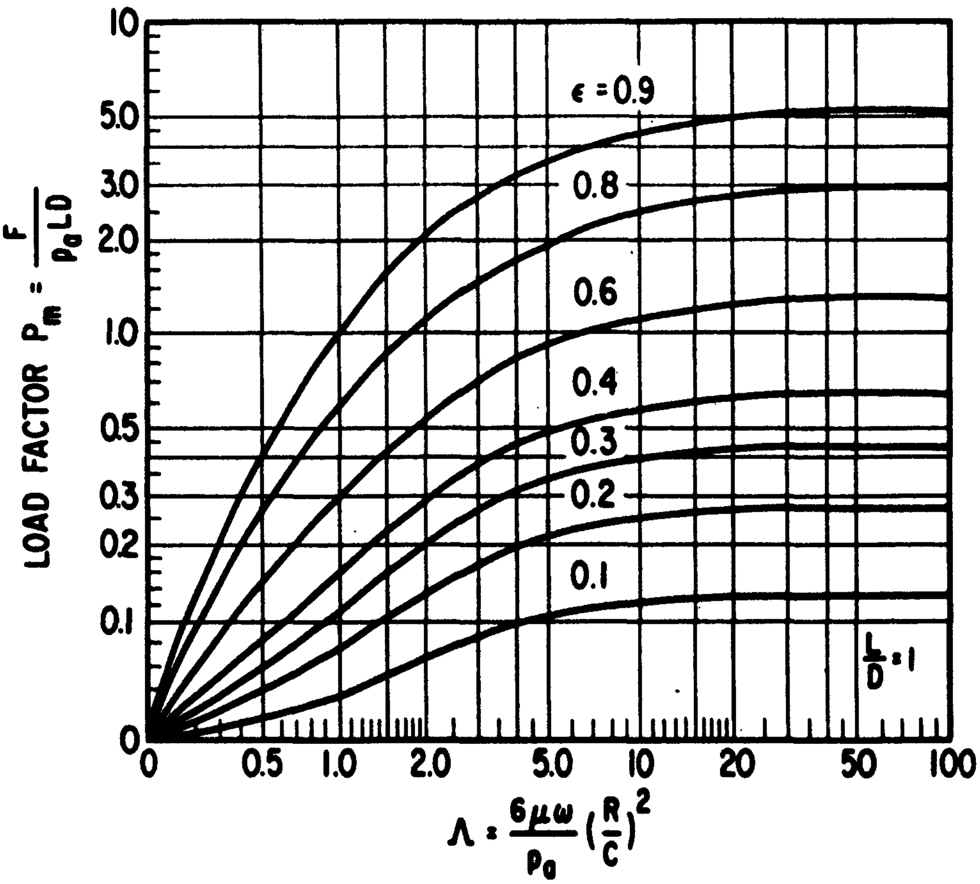

Figure 3 Load Chart for $\frac{L}{D} = 1$

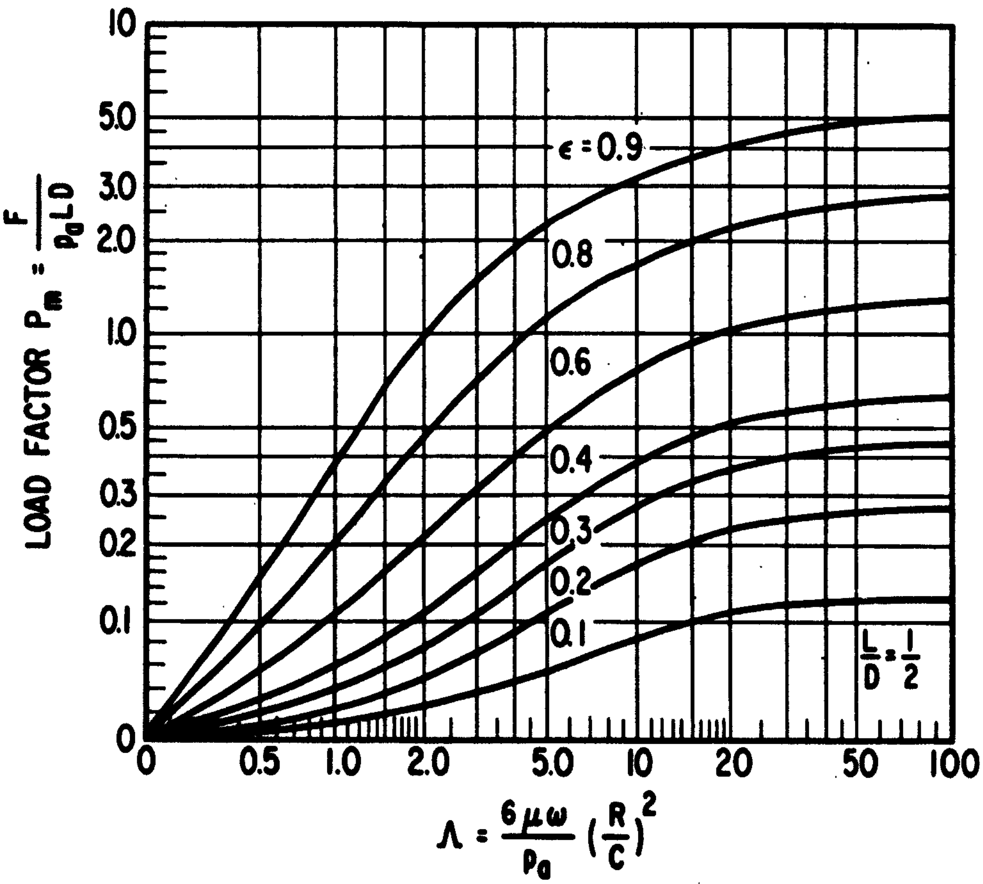

Figure 4 Load Chart for $\frac{L}{D} = 1/2$

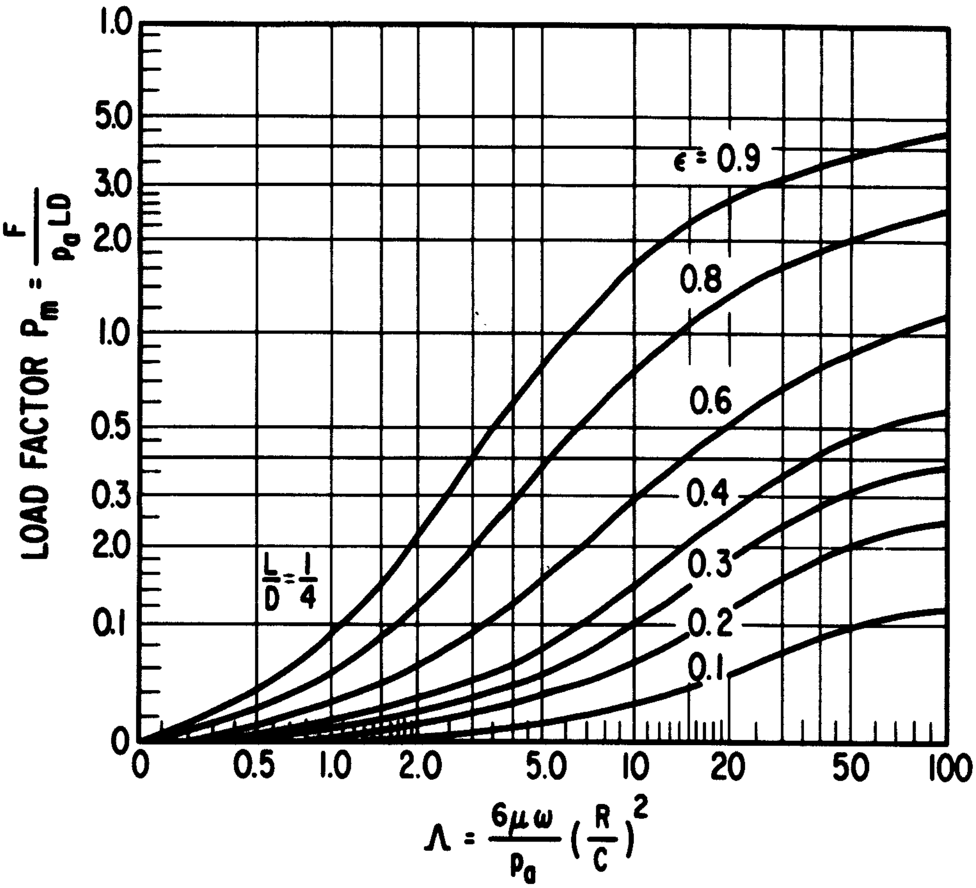

Figure 5 Load Chart for $\frac{L}{D}$ = 1/4

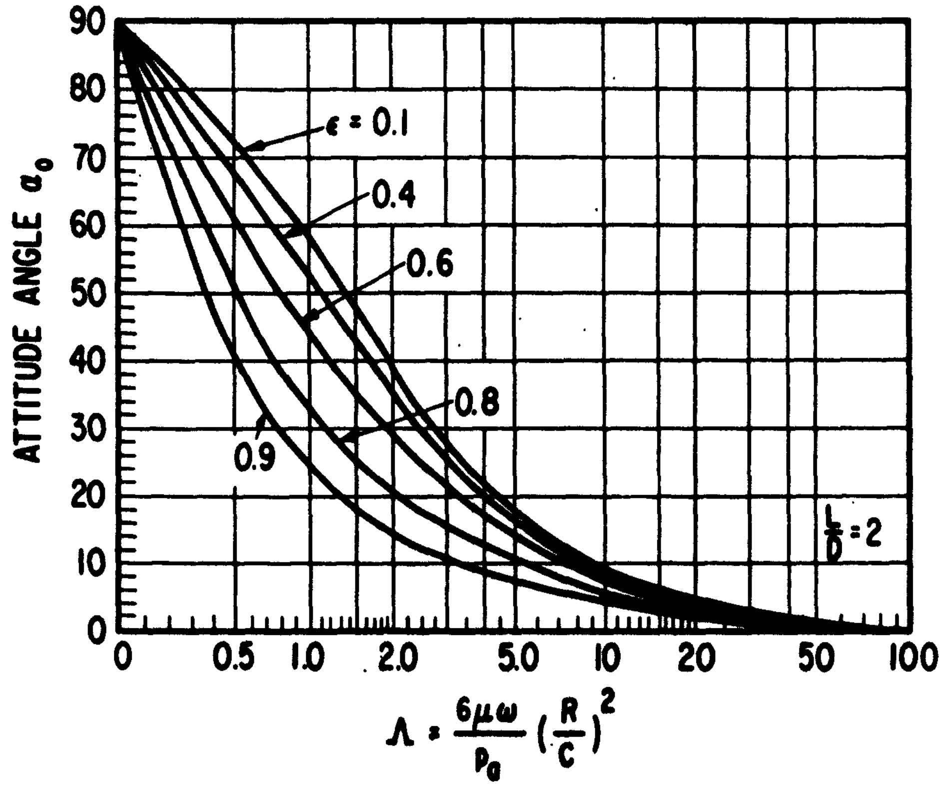

Figure 6 Attitude Angle Chart for $\frac{L}{D}$ = 2

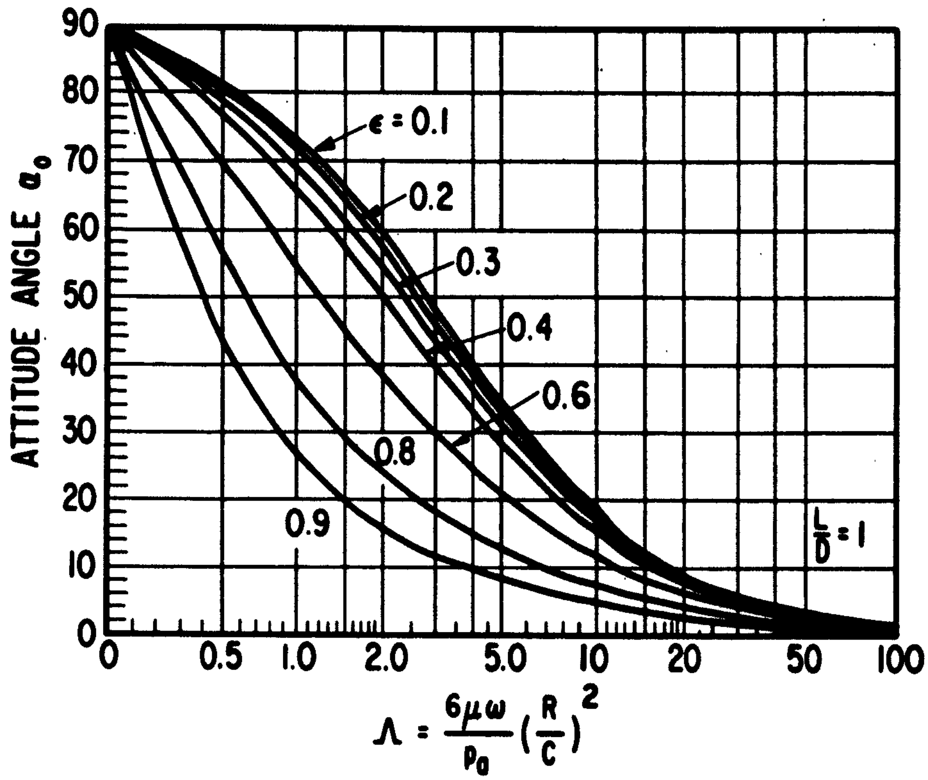

Figure 7 Attitude Angle Chart for $\frac{L}{D} = 1$

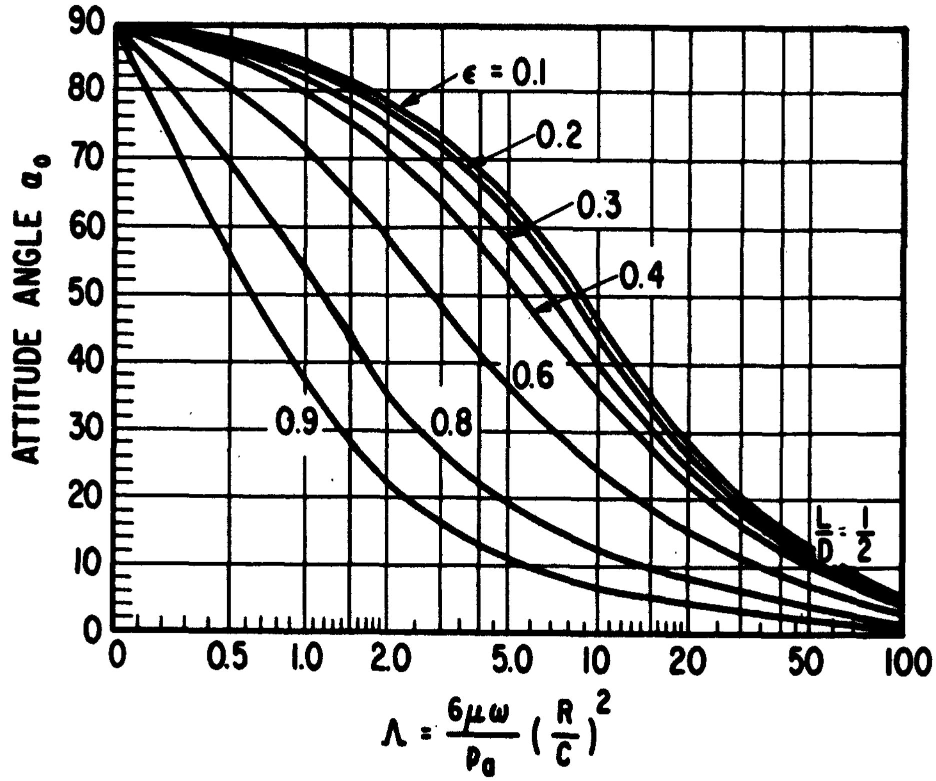

Figure 8 Attitude Angle Chart for $\frac{L}{D} = 1/2$

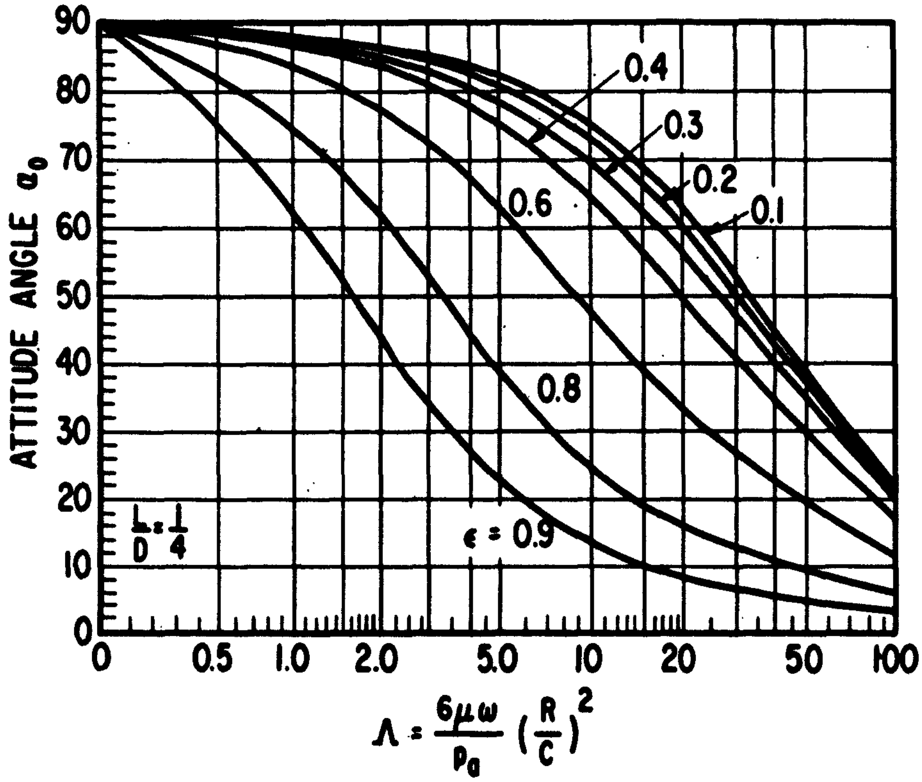

Figure 9 Attitude Angle Chart for $\frac{L}{D} = 1/4$

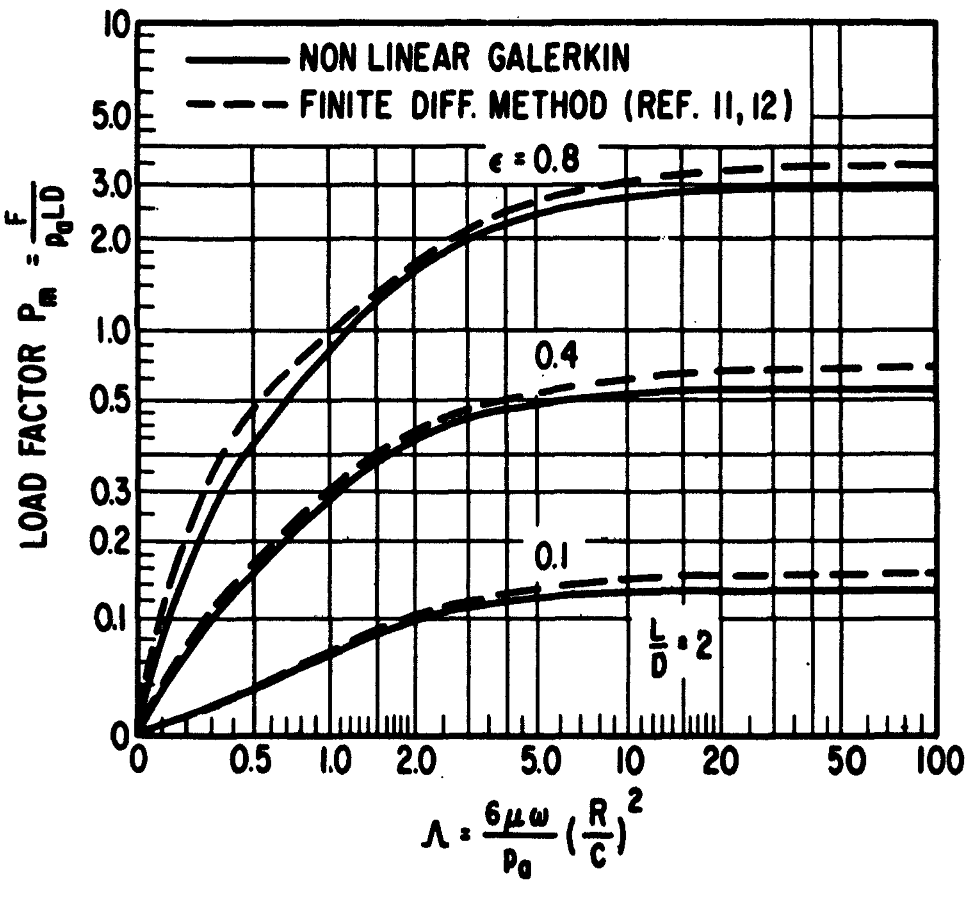

Figure 10 Comparison of Load Factors between Non-Linear Galerkin and Finite Difference Solutions for $\frac{L}{D} = 2$

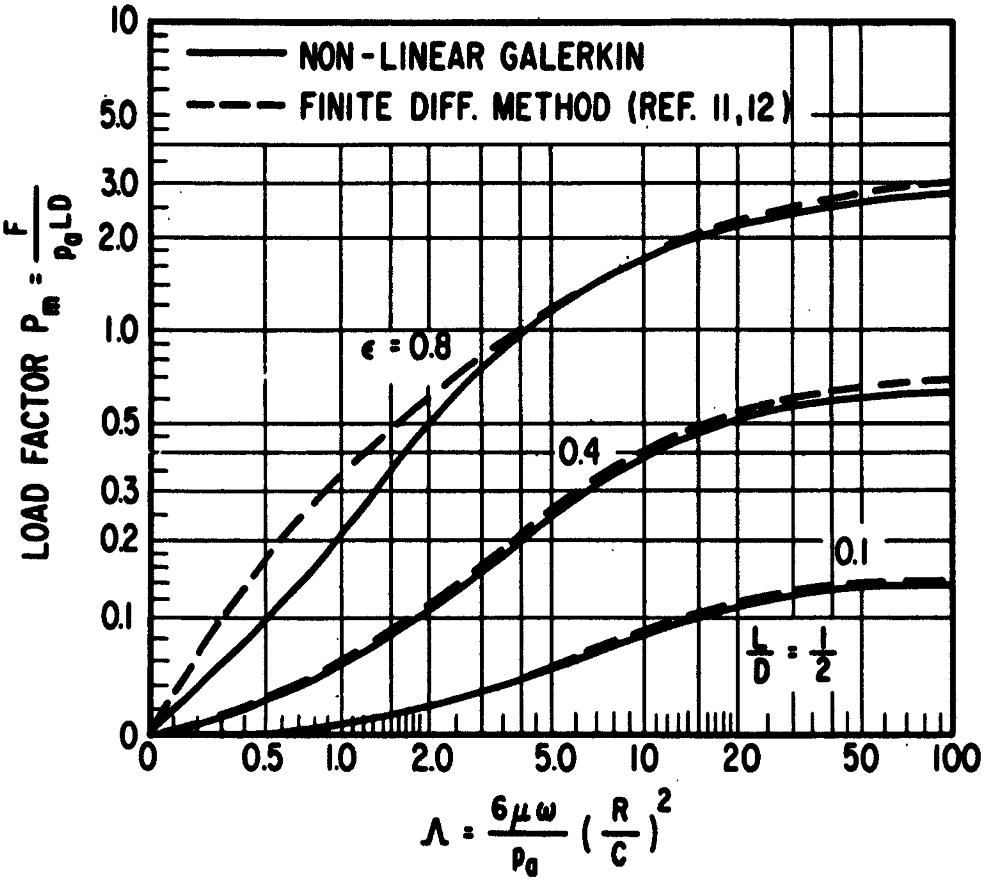

Figure 11 Comparison of Load Factors between Non-Linear Galerkin and Finite Difference Solutions for $\frac{L}{D} = 1/2$

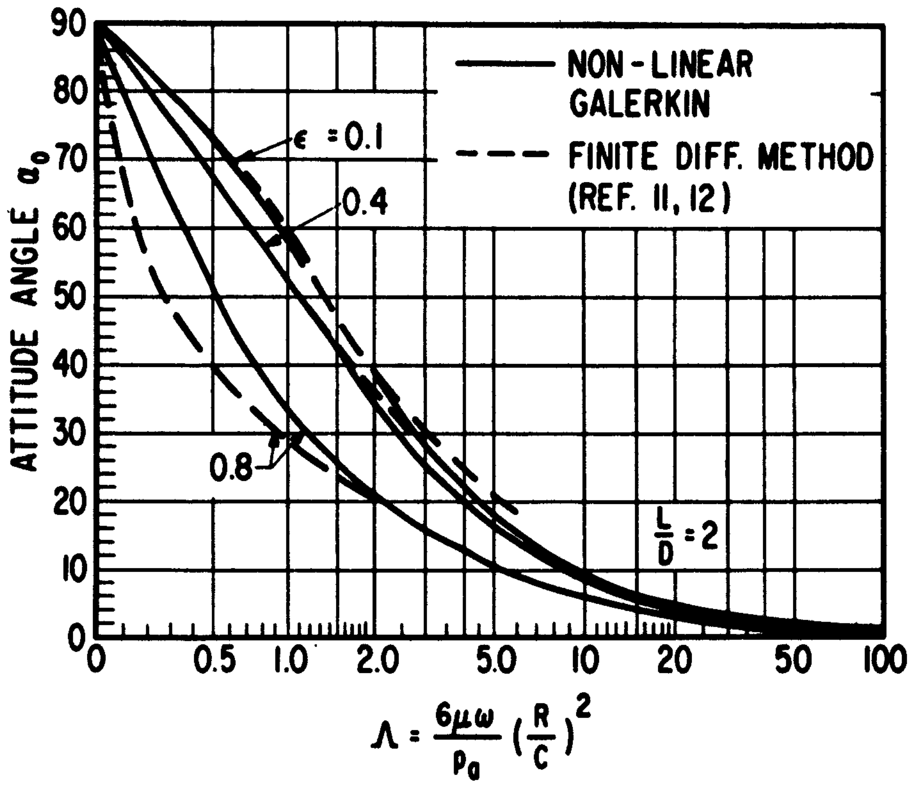

Figure 12 Comparison of Attitude Angles Between Non-Linear Galerkin and Finite Difference Solutions for $\frac{L}{D} = 2$

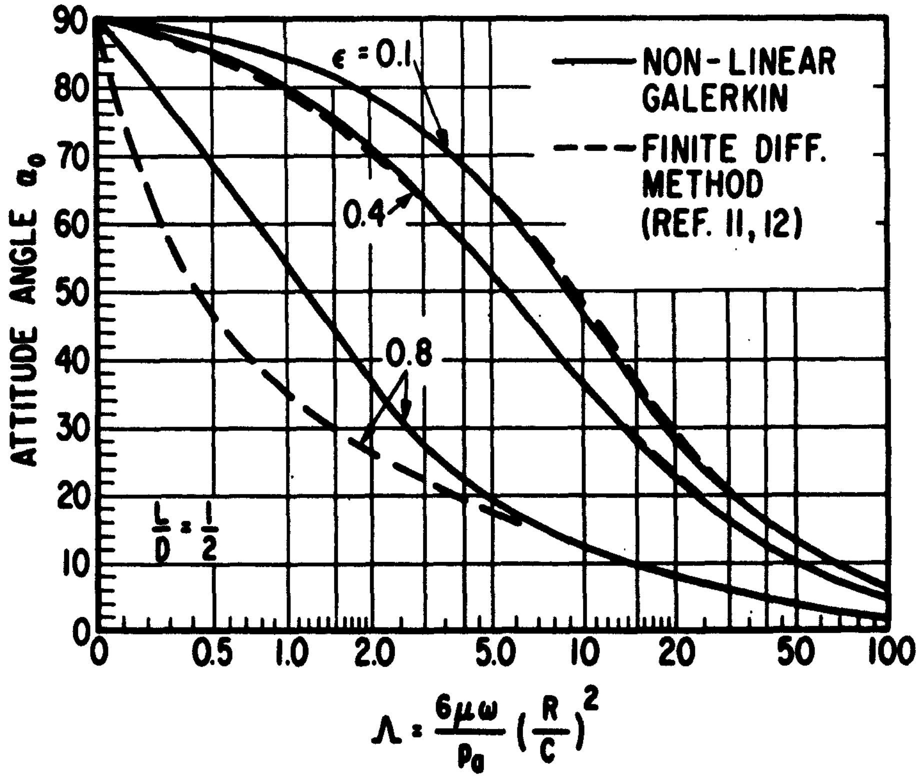

Figure 13 **Comparison of Attitude Angles Between Non-Linear Galerkin and Finite Difference Solutions for $\frac{L}{D} = 1/2$**

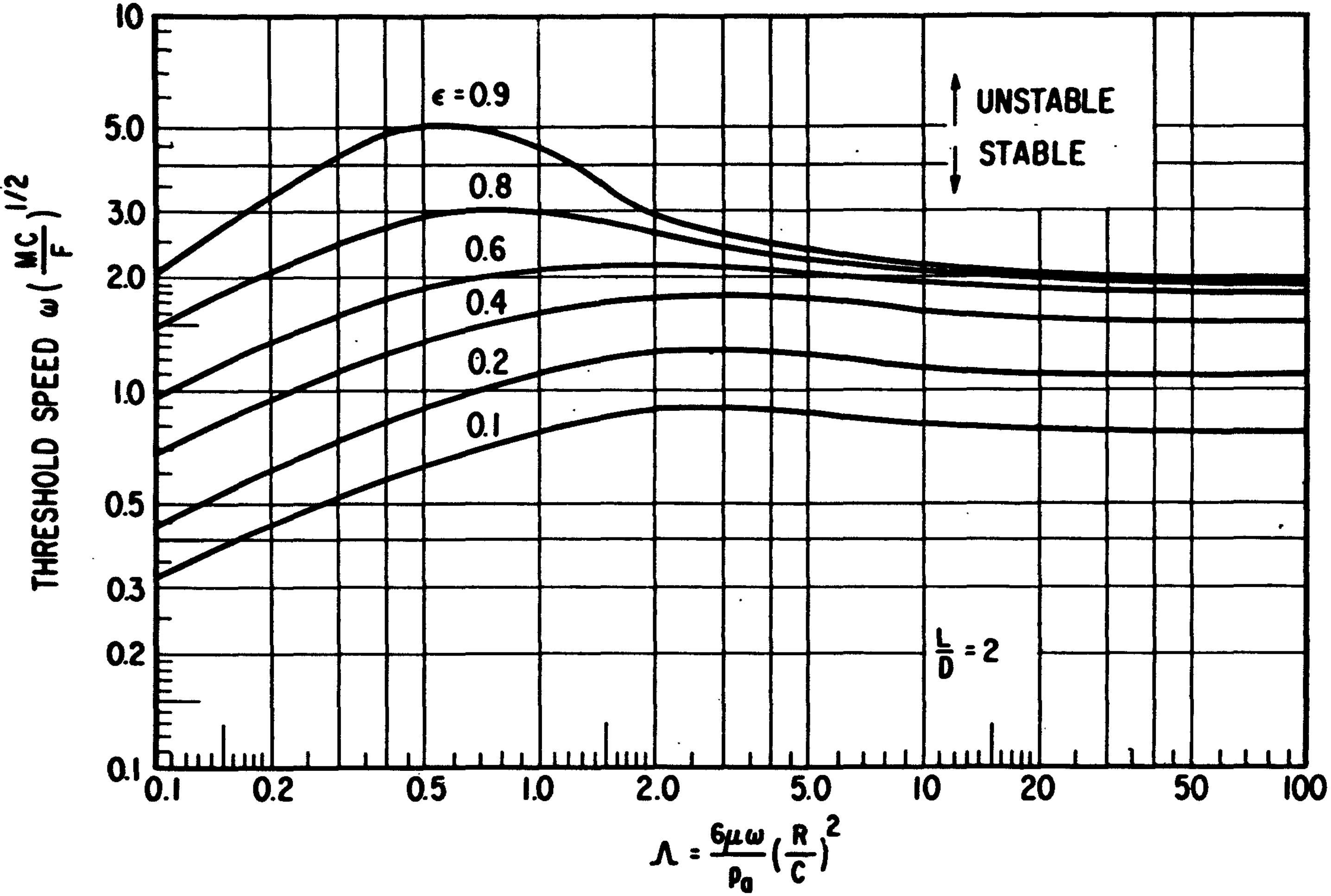

Figure 14 Stability Chart $\omega\left(\frac{MC}{F}\right)^{1/2}$ vs Λ for $\frac{L}{D} = 2$

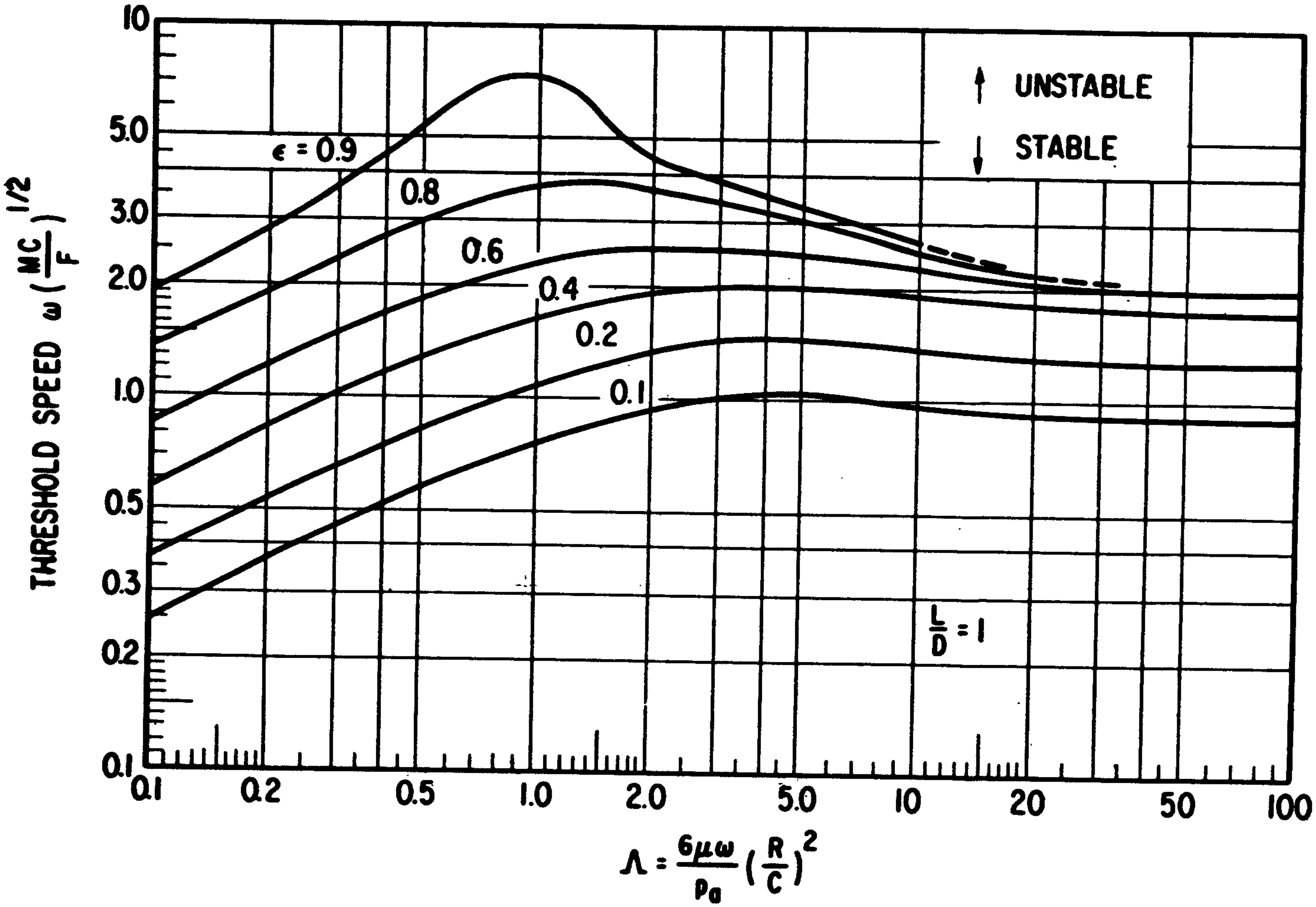

Figure 15 Stability Chart $\omega(\frac{MC}{F})^{1/2}$ vs Λ for $\frac{L}{D} = 1$

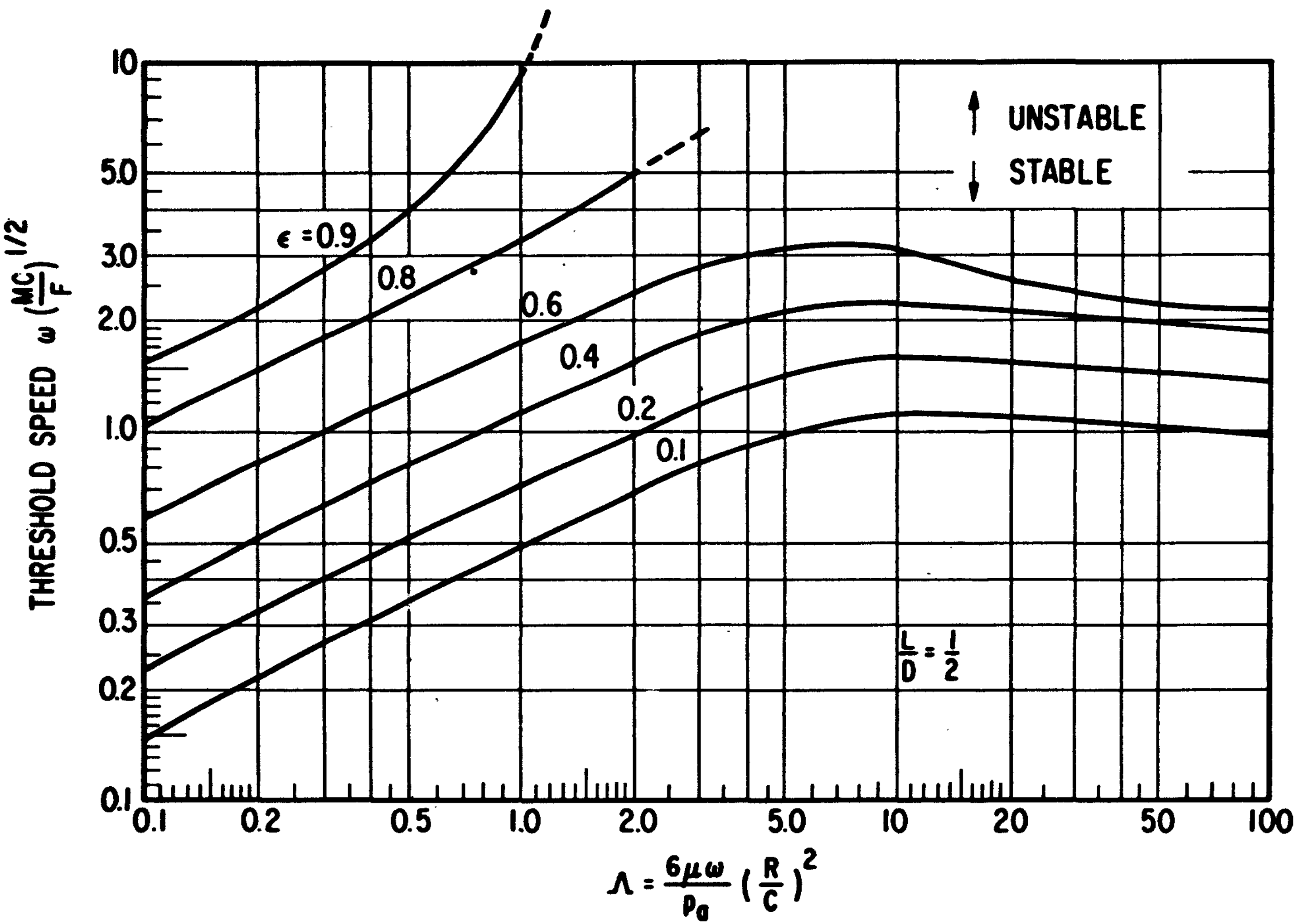

Figure 16 Stability Chart $\omega\left(\frac{MC}{F}\right)^{1/2}$ vs Λ for $\frac{L}{D} = 1/2$

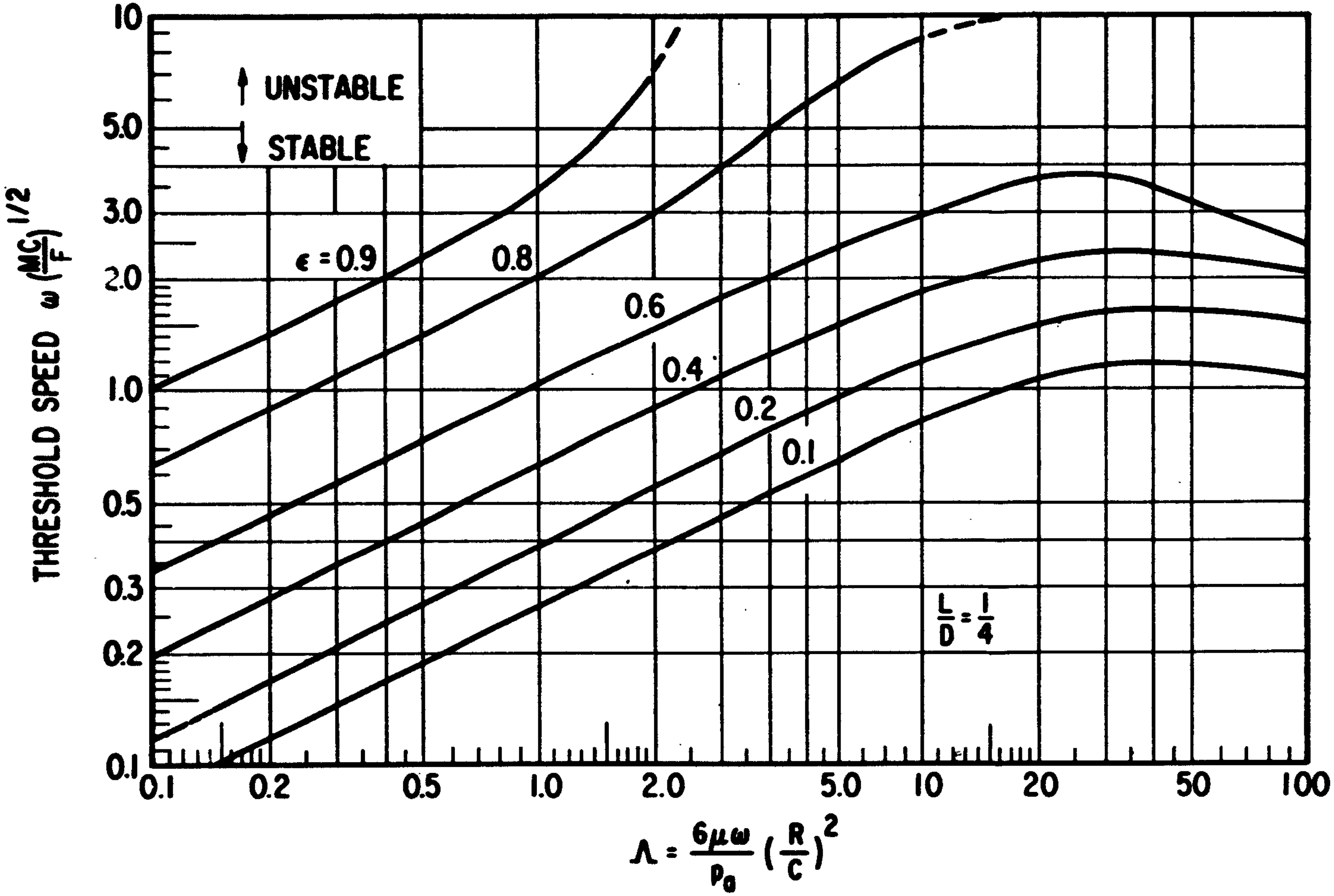

Figure 17 Stability Chart $\omega\left(\frac{MC}{F}\right)^{1/2}$ vs Λ for $\frac{L}{D} = 1/4$

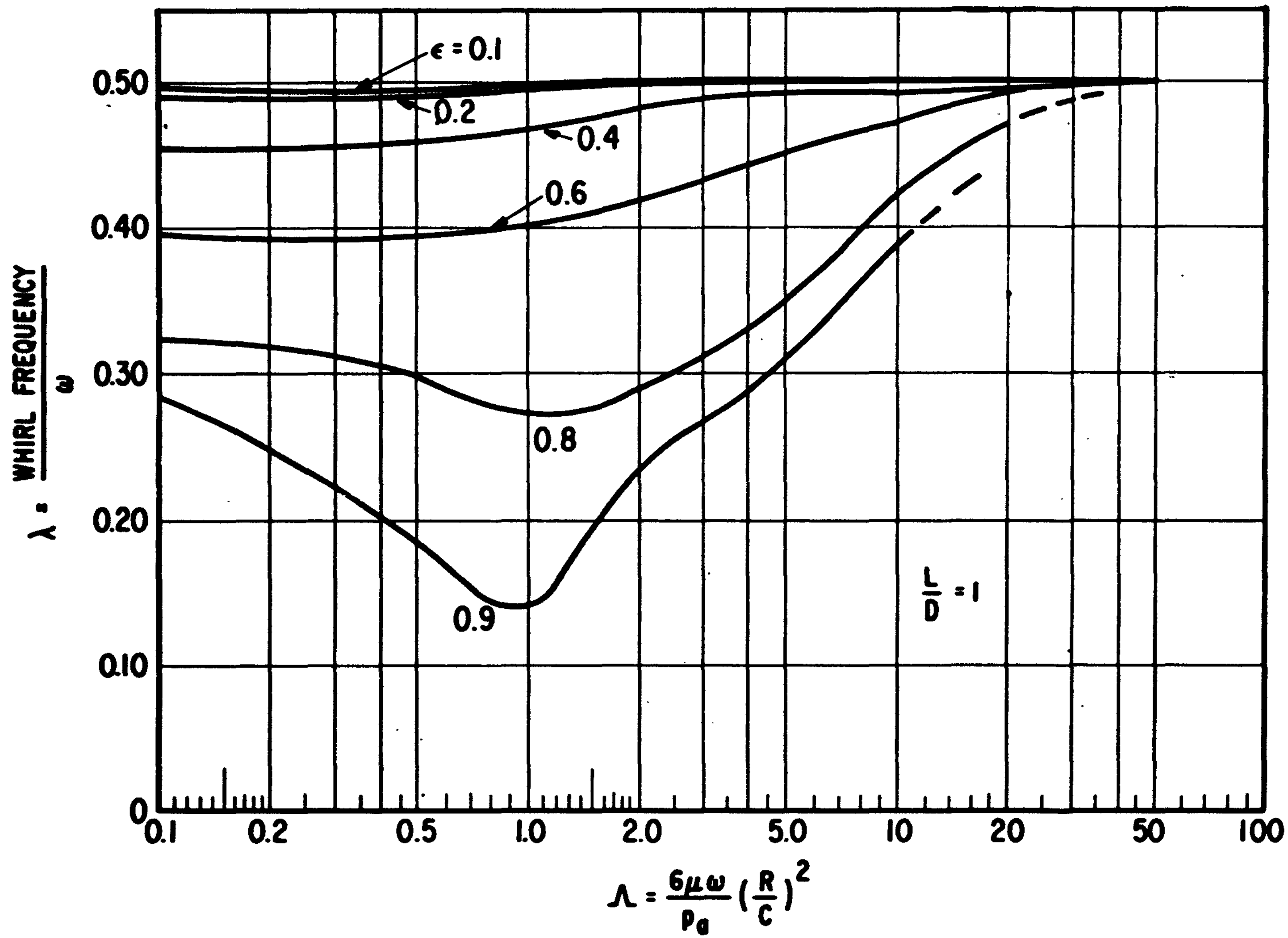

Figure 18 Whirl Frequency for $\frac{L}{D} = 1$

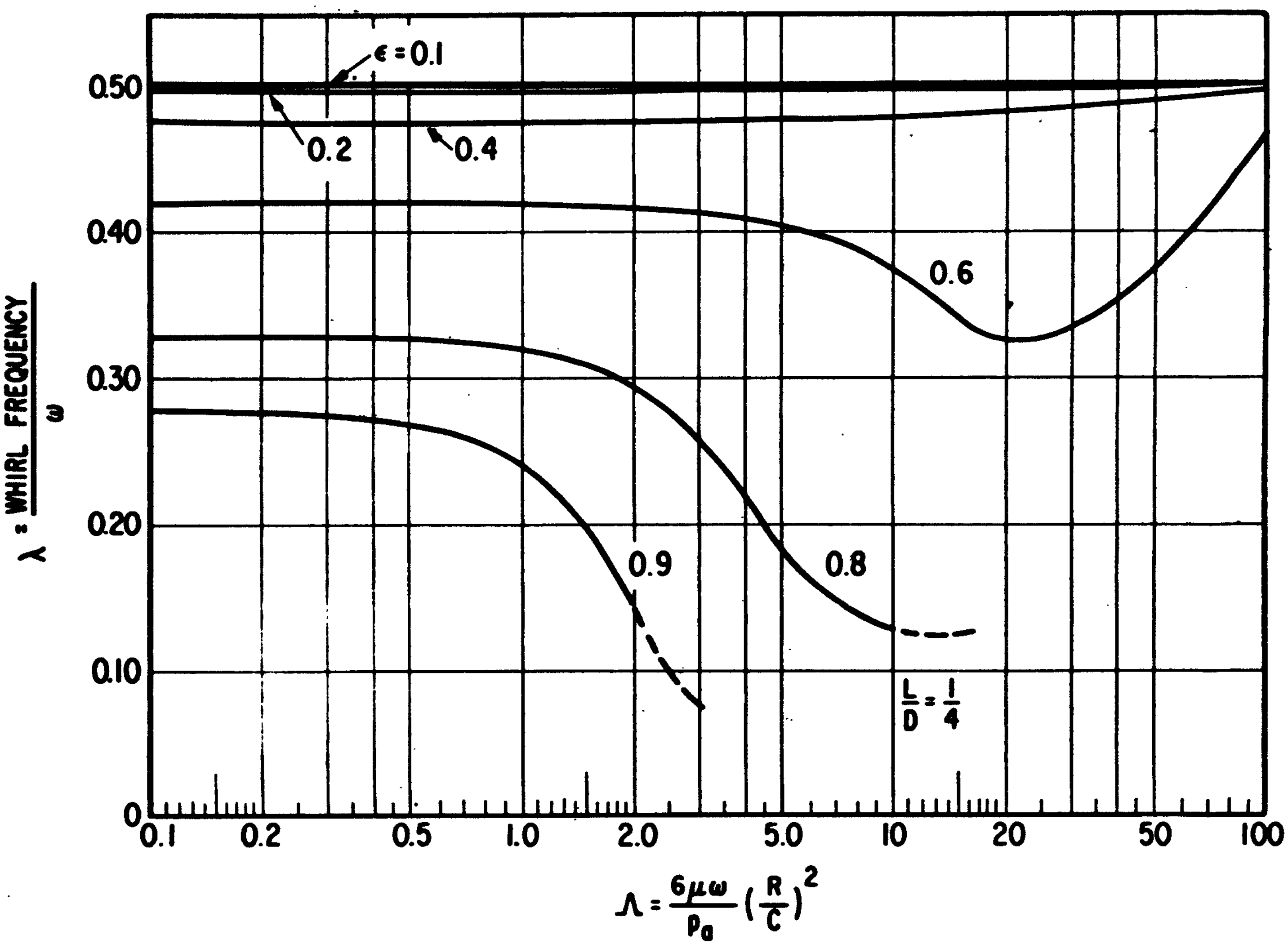

Figure 19 Whirl Frequency for $\frac{L}{D} = 1/2$

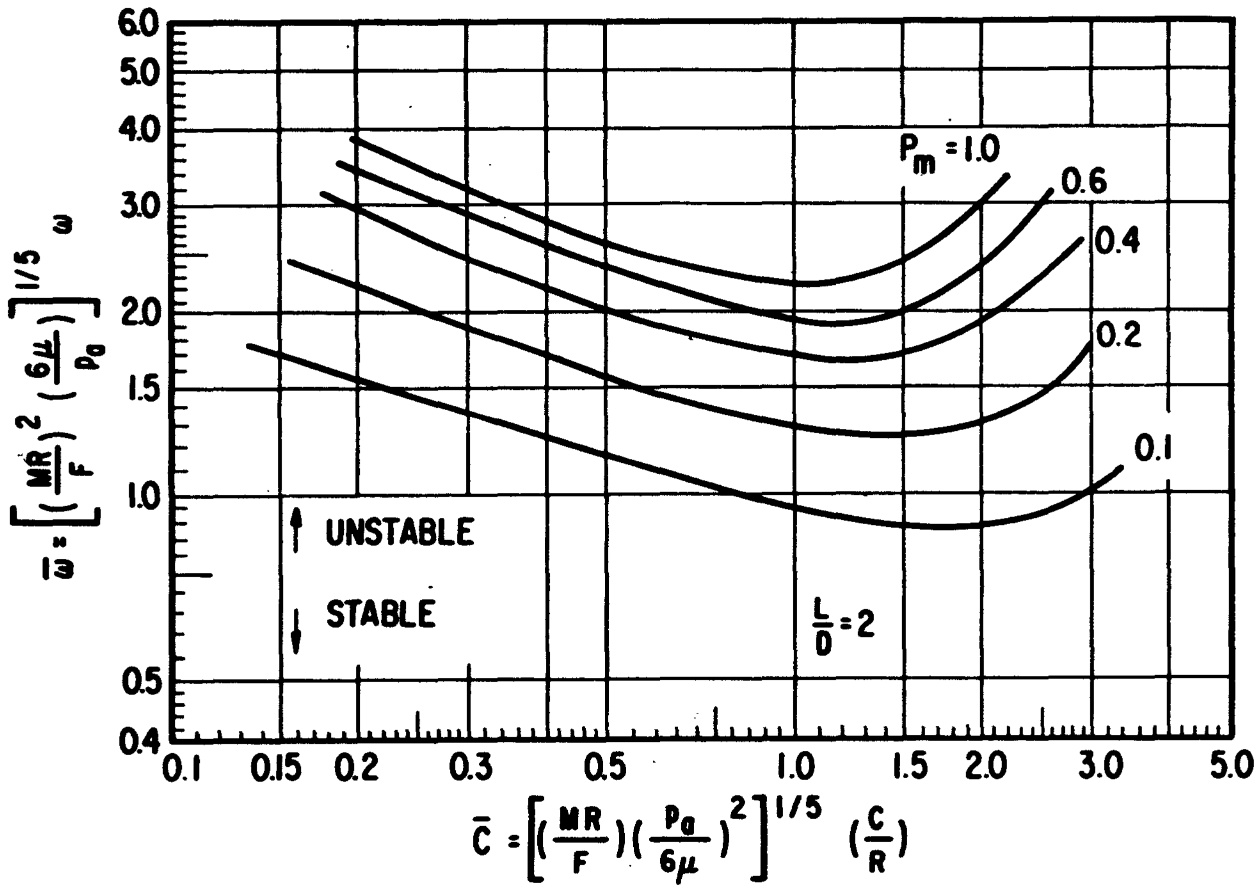

Figure 20 Stability Chart $\bar{C}$ vs $\bar{\omega}$ for $\frac{L}{D} = 2$

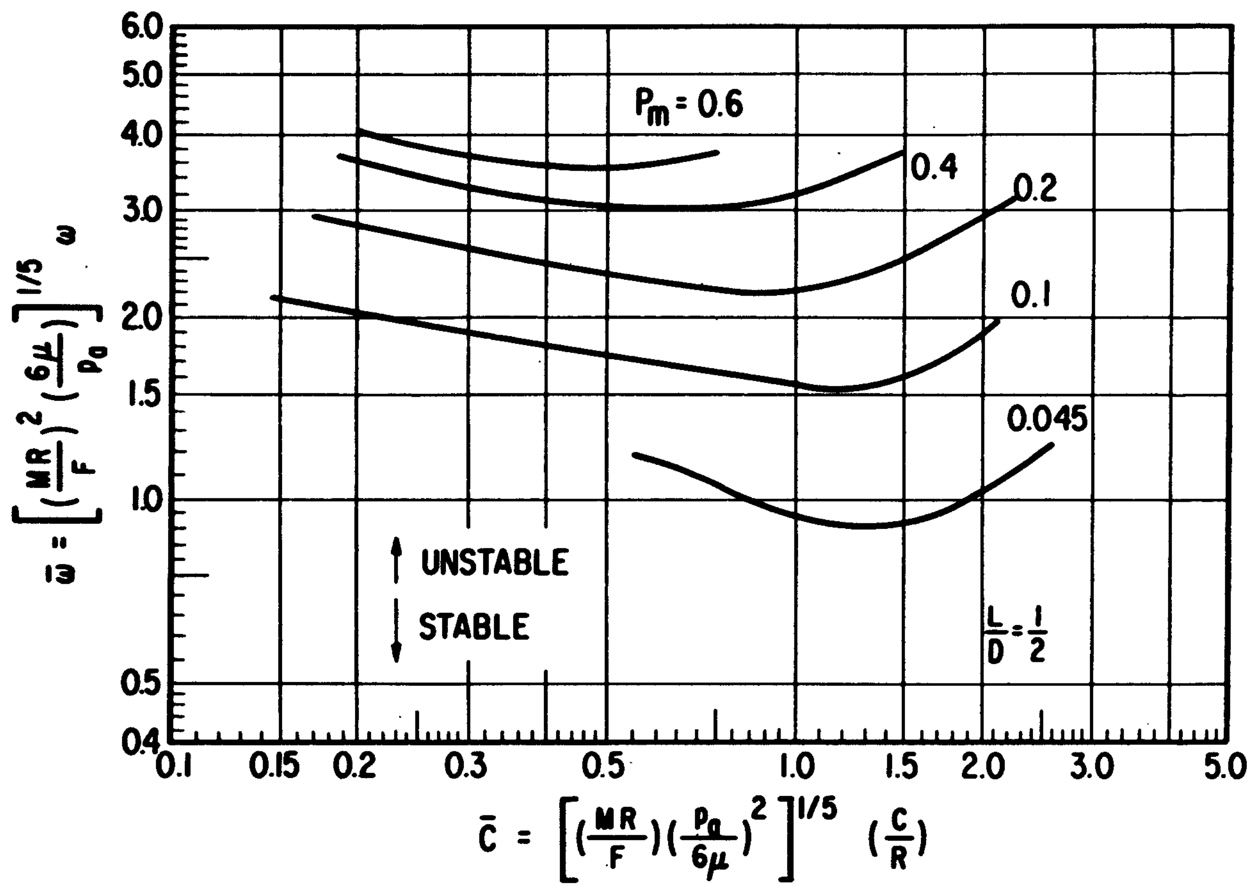

Figure 21 Stability Chart $\bar{C}$ vs $\bar{\omega}$ for $\frac{L}{D} = 1/2$

—□— NON-LINEAR GALERKIN $\frac{F}{p_a D^2} = 0.2$

— LINEARIZED PH-QUASI STATIC THEORY $\frac{F}{p_a D^2} = 0.2$

O DATA AFTER STERNLICHT - WINN $\frac{F}{p_a D^2} = 0.1873$

x DATA AFTER WHITLEY - BOWHILL - Mc EWAN $\frac{F}{p_a D^2} = 0.2$

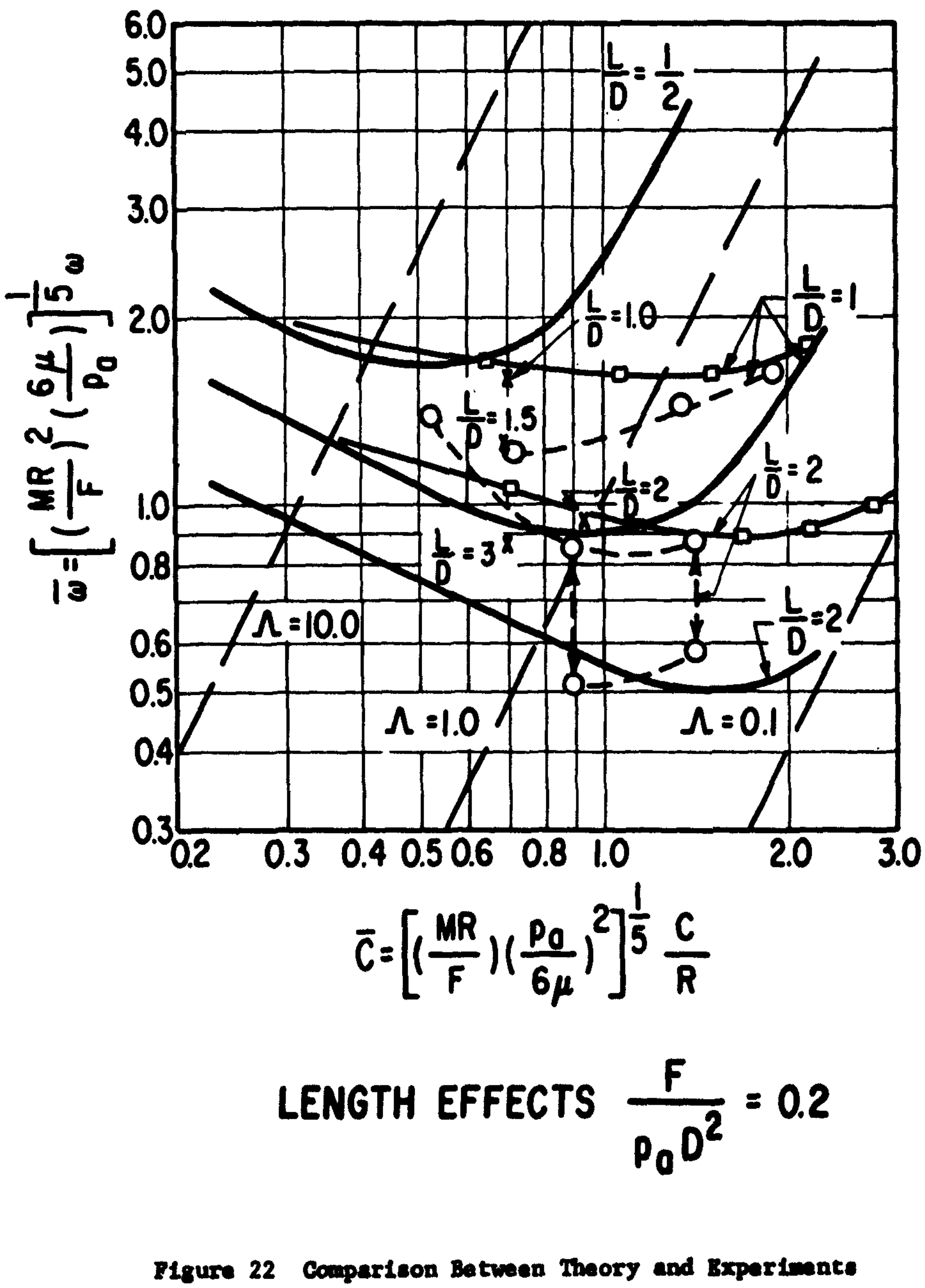

LENGTH EFFECTS $\frac{F}{p_a D^2} = 0.2$

Figure 22 Comparison Between Theory and Experiments

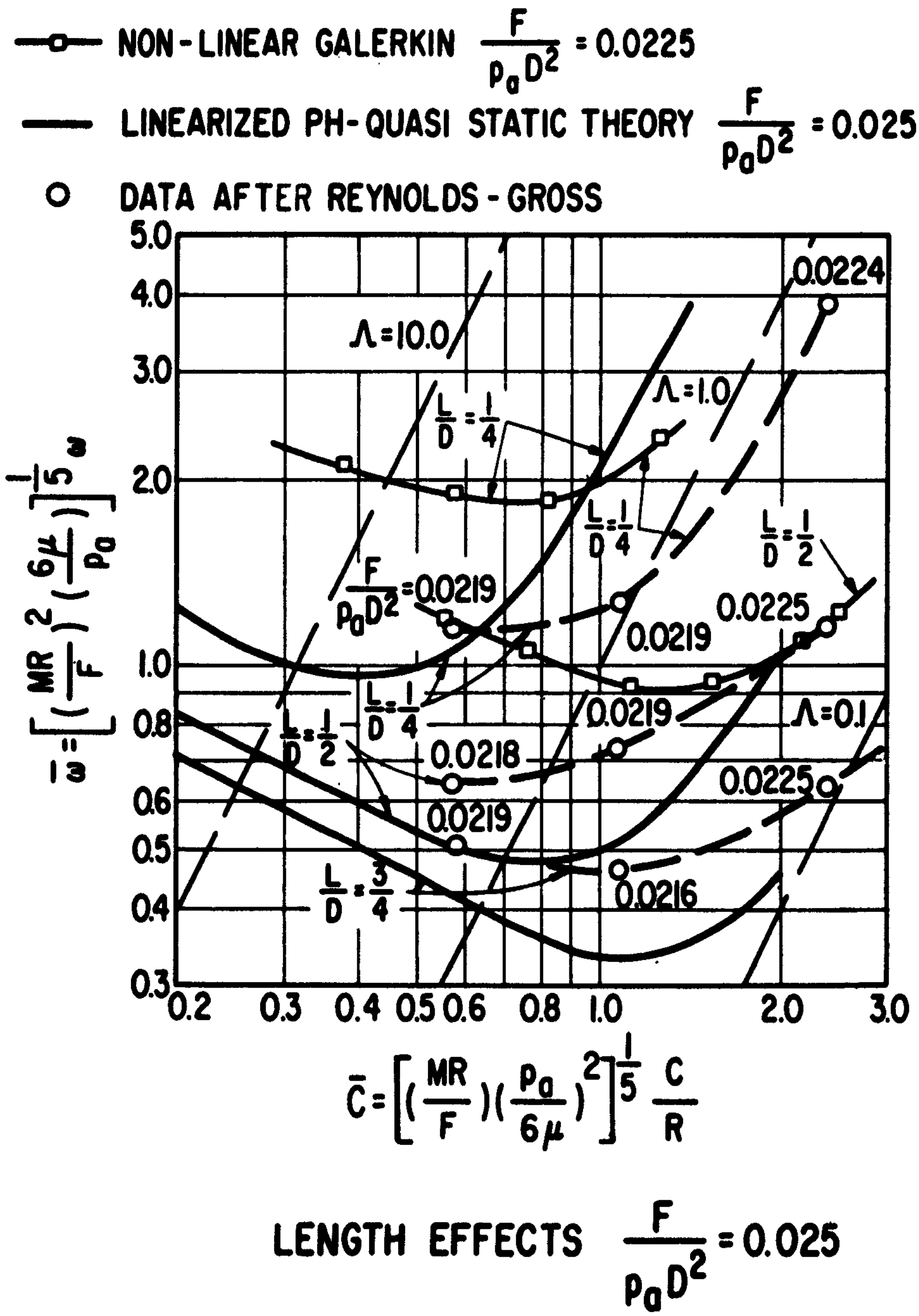

Figure 23 Comparison Between Theory and Experiments

APPROVED DISTRIBUTION LISTS FOR UNCLASSIFIED TECHNICAL REPORTS
ISSUED UNDER
GAS LUBRICATED BEARINGS CONTRACTS

Contract ____________ NR ______

Chief of Naval Research
Department of the Navy
Washington 25, D. C.
Attn: Codes 438 5
429 1
461 1
463 1
466 1

Commanding Officer
Office of Naval Research
Branch Office
495 Summer Street
Boston 10, Massachusetts 1

Commanding Officer
Office of Naval Research
Branch Office
86 East Randolph Street
Chicago 1, Illinois 1

Commanding Officer
Office of Naval Research
Branch Office
207 West 24th Street
New York 11, New York 1

Commanding Officer
Office of Naval Research
Branch Office
1000 Geary Street
San Francisco 9, California 1

Commanding Officer
Office of Naval Research
Branch Office
1030 East Green Street
Pasadena 1, California 1

Commanding Officer
Office of Naval Research
Branch Office
Box 39, Navy #100
Fleet Post Office
New York, New York 10

Chief, Bureau of Ships
Department of the Navy
Washington 25, D. C.
Attn: Code 644B (James C. Reid, Jr.) 1
342 (E. A. Bukzin) 1
634 (E. A. Vagman) 1

Chief, Bureau of Naval Weapons
Department of the Navy
Washington 25, D. C.
Attn: Codes RRMN-431 (J. W. Case) 1
RADP-4 (S. Collegeman) 1

Director
Naval Research Laboratory
Washington 25, D. C.
Attn: Code 2000 6
5230 1

Special Projects Office
Department of the Navy
Washington 25, D. C.
Attn: Code SP23-A (D. Gold) 1

Head, Bearings and Seals Branch
U. S. Naval Engineering Experiment Station
Annapolis, Maryland
Attn: Code 851 (Watt V. Smith) 1
Mr. Robert Belt 1

Material Laboratory Library
Building 291, Code 912B
New York Naval Shipyard
Brooklyn 1, New York 1

Library
Technical Reports Section
U. S. Naval Postgraduate School
Monterey, California 1

Commanding Officer
U. S. Naval Avionics Facility
Indianapolis 18, Indiana
Attn: J. G. Weir 1

Director
U. S. Naval Boiler and Turbine Lab.
Naval Base
Philadelphia 12, Pennsylvania 1

Office of Chief of Ordnance
Research and Development Division
Department of the Army
Washington 25, D. C.
Attn: Norman L. Klein 1

Fuels & Lubricants Section
Research Branch
Research & Development Division
Office, Chief of Ordnance
Attn: Mr. Ronald E. Streets
4th Floor, Pentagon Annex #2
Washington 25, D. C. 1

Chief of Research and Development
Office, Chief of Staff
Department of the Army
Pentagon Building
Washington 25, D. C. 1

Commanding General
U. S. Army Engineer R&D Laboratories
Fort Belvoir, Virginia
Attn: W. M. Crim, Nuclear Power Field Office 2

Director U. S. Army Engineer Research and Development Laboratory
Fort Belvoir, Virginia
Attn: Technical Documents Center 1

Commander
Army Rocket & Guided Missile Agency
Redstone Arsenal, Alabama
Attn: Technical Library 1

ESD - AROD
Box CM, Duke Station
Durham, North Carolina 1

Chief of Staff, U. S. Air Force
The Pentagon
Washington 25, D. C.
Attn: AFRDR-AS/M 1

Commander
Air Force Office of Scientific Research
Washington 25, D. C.
Attn: SRHM 1

Commander
Aeronautical Systems Division
of the Air Force Systems Command
Wright-Patterson AF Base, Ohio
Attn: ASRCNL-2, J. L. Morris 2
ASRMDD, F. D. Hanlon 1
ASRMFP-1, B. L. McFadden, Jr. 1
ASRMOCO-1, R. W. McAdory 1
Mr. G. A. Peane 1

Armed Services Technical Information Agency
Arlington Hall Station
Arlington 12, Virginia 10

Office of Assistant Director (Army Reactors)
Division of Reactor Development
U. S. Atomic Energy Commission
Washington 25, D. C.
Attn: Mr. Clarence E. Miller, Jr. 2

Mr. N. Grossman, Chief
Engineering Development Branch
Reactor Development Division
U. S. Atomic Energy Commission
Washington 25, D. C. 1

Headquarters Library
U. S. Atomic Energy Commission
Washington, D. C. 1

Chief, Division of Engineering
Maritime Administration
GAO Building
Washington 25, D. C. 1

Cryogenic Engineering Laboratory
National Bureau of Standards
Boulder, Colorado
Attn: Library 1

Mr. Harold Hessing
National Aeronautics and Space Administration
1512 H. Street, N. W.
Washington 25, D. C. 2

Mr. Edmund E. Bisson
Chief, Lubrication & Wear Branch
Lewis Research Center
National Aeronautics and Space Administration
21000 Brookpark Road
Cleveland, Ohio 1

Mr. Rudolph H. Beyer
George C. Marshall Space Flight Center
National Aeronautics and Space Administration
Guidance and Control Division
Gyro-Stabilizer Branch
Huntsville, Alabama 12

Mr. H. W. Savage
Oak Ridge National Laboratory
Post Office Box Y
Oak Ridge, Tennessee 1

Chief, Technical Information Service Extension
P. O. Box 62
Oak Ridge, Tennessee
Attn: Melvin S. Day 1

Applied Physics Laboratory
Johns Hopkins University
Silver Spring, Maryland
Attn: George L. Seielstad, Supr., Tech., Reports Group 1

Department of Chemical Engineering
New York University
New York 53, New York
Attn: James J. Barker, Assoc., Prof. of Nuclear Engineering 1

Professor A. Charnes
The Technological Institute
Northwestern University
Evanston, Illinois 1

Resident Representative
Office of Naval Research
c/o University of Pennsylvania
3438 Walnut Street
Philadelphia 4, Pennsylvania 1

Professor P. R. Trumpler
Towne School of Civil and Mechanical Engineering
University of Pennsylvania
Philadelphia, Pennsylvania 1

Jet Propulsion Laboratory
California Institute of Technology
4800 Oak Grove Avenue
Pasadena, California
Attn: Mr. Norri Sirri 1
Library 1

Illinois Institute of Technology
Chicago 16, Illinois
Attn: Professor L. N. Tao 1

Professor M. C. Shaw, Head
Department of Mechanical Engineering
Carnegie Institute of Technology
Pittsburgh 13, Pennsylvania 1

Engineering Projects Laboratory
Massachusetts Institute of Technology
Cambridge 39, Massachusetts
Attn: Dr. R. W. Mann (Room 3-459 A) 1

Massachusetts Institute of Technology
Instrumentation Laboratory
68 Albany Street
Cambridge 39, Massachusetts
Attn: Library, W1-109 1

Professor F. F. Martinuzzi
Stevens Institute of Technology
Hoboken, New Jersey 1

Battelle Memorial Institute
505 King Avenue
Columbus 1, Ohio
Attn: Dr. Russell Dayton 1

Franklin Institute
Laboratory for Research and Development
Philadelphia, Pennsylvania
Attn: Professor D. D. Fuller 3

Library Institute of Aerospace Sciences
2 East 64th Street
New York, New York 1

Mr. O. B. Speen
Sr. Member, Technical Staff
ITT Federal Laboratories
Division of International Telephone and Telegraph Corporation
15151 Bledsoe Street
San Fernando, California 1

Aerojet-General Nucleonics
P. O. Box 86
San Ramon, California
Attn: Barbara M. Probert 1

Aerospace Corporation
P. O. Box 95085
Los Angeles 45, California
Attn: Aerospace Library 1
Technical Reports Group 1

AiResearch Manufacturing Company
Sky Harbor Airport
402 South 36th Street
Phoenix, Arizona
Attn: Librarian 1

Mr. William D. Stimmel
Research Laboratories Library
Allis-Chalmers Manufacturing Company
Milwaukee 1, Wisconsin 1

J. W. Fecker Division
American Optical Company
4709 Baum Blvd.
Pittsburgh 13, Pennsylvania 1

American Society of Lubrication Engineers
5 North Wabash Avenue
Chicago 2, Illinois 1

Chairman
Research Committee on Lubrication
The American Society of Mechanical Engineers
United Engineering Center
345 East 47th Street
New York 17, New York 2

Mr. James R. Kerr, President
Lycoming Division
AVCO
Stratford, Connecticut 1

Research Precision Mechanisms
Division of the Barden Corporation
4 Old Newtown Road
Danbury, Connecticut
Attn: D. L. Mims, Vice President - General Manager 1

Beemer Engineering Company
Industrial Park
Fort Washington, Pennsylvania 1

Utica Division
The Bendix Corporation
211 Seward Avenue
Utica, New York
Attn: Mr. Russell T. DeMuth, Supervisory Engineer 1

Bendix Aviation Corporation
Research Laboratories Division
Southfield, Michigan
Attn: Mr. Ralph A. Larson 1

Mr. C. R. Adams
Physics Technology Department
Aero-Space Division
The Boeing Company
Seattle 24, Washington 1

Bryant Chucking Grinder Company
60 Clinton Avenue
Springfield, Vermont
Attn: Mr. Raold Cann 1

Cadillac Gage Company
P. O. Box 3806
Detroit 5, Michigan
Attn: Mr. J. Taylor, Project Manager 1

Dr. Dewey J. Handell
Director of Development
Carrier Research and Development Co.
Carrier Parkway
Syracuse, New York 1

Chance Vought Corporation
P. O. Box 5907
Dallas, Texas
Attn: Mr. R. C. Blaylock, Vice President (Engineering) 1

Chrysler Corporation
Defense Operations
P. O. Box 757
Detroit 31, Michigan
Attn: Mr. C. W. Snider 1

J. D. Hammerchev & Associates
Consulting Engineers
3900 Main Street
Houston 2, Texas 1

Mr. D. V. Birmingham
Cryogenic Engineering Laboratory
National Bureau of Standards
Boulder, Colorado 2

Curtiss Wright Corporation
Wright Aeronautical Division
Department 8332
Wood Ridge New Jersey
Attn: W. J. Derner, Chief Project Engineer 1

Page 5

Daystrom Pacific
9320 Lincoln Boulevard
Los Angeles 45, California
Attn: Robert E. Smith
Special Project Engineer 1

Ford Instrument Company
31-10 Thomson Avenue
Long Island City 1, New York
Attn: Mr. Jarvis 1

Mr. Adolf Egli
Ford Motor Company
Engineering and Research Staff
P. O. Box 2053
Dearborn, Michigan 1

Dr. John E. Mayer, Jr.
Non-Metallics Section
Applied Science Department
Scientific Laboratory
Ford Motor Company
P. O. Box 2053
Dearborn, Michigan 1

AiResearch Manufacturing Division
The Garrett Corporation
9851 S. Sepulveda Boulevard
Los Angeles, California
Attn: Jerry Glaser, Supervisor
Mechanical Lab. -Dept. 93-17 1

General Atomics Division
General Dynamics Corporation
P. O. Box 608
San Diego 12, California
Attn: Mr. F. W. Simpson 1

Bearing and Lubricant Center
General Engineering Laboratory
General Electric Company
1 River Road
Schenectady, New York
Attn: G. R. Fox, Manager 2

Mr. L. W. Winn
General Electric Company
Aircraft Accessory Turbine Department
950 Western Avenue, Bldg. 3-74
Lynn, Massachusetts 1

Research Laboratories
General Motors Corporation
General Motors Technical Center
12 Mile and Mound Roads
Warren, Michigan
Attn: Mr. E. Roland Maki,
Mechanical Development Dept. 1

A. C. Spark Plug Division
General Motors Corporation
Milwaukee 1, Wisconsin
Attn: Allen Knudsen 1

Mr. Walter Carow
Kearfott Division
General Precision Inc.
1150 McBride Avenue
Little Falls, New Jersey 1

Grumman Aircraft Engineering Corp.
Bethpage, Long Island, New York
Attn: Mr. David W. Craig, Jr.
Mechanical Design Section
Engineering Department 1

Hydronautics, Incorporated
Pindell School Road
Howard County
Laurel, Maryland 1

International Business Machines Corp.
Research Laboratory
San Jose, California
Attn: Dr. W. E. Langlois 2

Mr. L. R. Barr, V. P.
Lear-Romec Division
Abbe Road
Elyria, Ohio 1

Dr. Calus G. Goetzel, D/53-30
Bldg. 201, Plant 2, Palo Alto
Lockheed Missiles & Space Co.
P. O. Box 504
Sunnyvale, California 1

Page 6

Dr. J. B. Ausman
Litton Systems, Inc.
5500 Canoga Avenue
Woodland Hills, California 2

Mr. Don Moore
Litton Systems
5500 Canoga Avenue
Woodland Hills, California 1

Mr. A. E. Thomas
Astro Division
The Marquardt Corporation
16555 Saticoy Street
Van Nuys, California 1

Mr. Kendall Perkins
Vice President (Engr)
McDonnell Aircraft Corporation
Lambert St. - St. Louis
Municipal Airport
Box 516
St. Louis 3, Missouri 1

Dr. Beno Sternlicht
Mechanical Technology Incorporated
1 Herbert Drive
Latham, New York 3

Mr. J. W. Lower
Chief, Engineer-Inertial Components
Honeywell Aero Division
2600 Ridgway Road
Minneapolis, Minnesota 1

Mr. Carl F. Graesser, Jr.
Director of Research
New Hampshire Ball Bearings, Inc.
Peterborough, New Hampshire 1

Mrs. Alice Ward, Librarian
Norden Division of United Aircraft Corp.
Helen Street
Norwalk, Connecticut 1

Northrop Corporation
Norair Division
1001 East Broadway
Hawthorne, California
Attn: Technical Information, 3125 1

Mr. N. L. Simmons
Nortronics
A Division of Northrop Corporation
500 East Orangethorpe Avenue
Anaheim, California 1

Nortronics
A Division of Northrop Corporation
100 Morse Street
Norwood, Massachusetts
Attn: Mr. E. L. Swainson, Tech. Asst.
Precision Products Department 1

Pratt & Whitney Aircraft
Division of UAC - CANEL
P. O. Box 611
Middletown, Connecticut
Attn: Librarian 1

Library, Bldg. 10-2-5
Radio Corporation of America
Camden 2, New Jersey 1

Mr. Robert S. Siegler
Rocketdyne
Nucleonics Subdivision
6633 Canoga Avenue
Canoga Park, California 2

Ryan Aeronautical Company
Attn: Engineering Library
Lindbergh Field
San Diego 12, California 1

Mr. M. A. Vreeland
Sanderson & Porter
72 Wall Street
New York 5, New York 1

Jack & Heintz, A Division of
The Siegler Corporation
1725 Eye Street, Suite 505
Washington 6, D. C. 1

Mr. Paul A. Pitt, Vice President
Engineering & Research
Solar Aircraft Company
2200 Pacific Highway
San Diego 12, California 1

Mr. W. G. Wing
Sperry Gyroscope Company
C-2
Great Neck, New York 1

Page 7

Mrs. Florence Turnbull
Engineering Librarian
Sperry Gyroscope Company
Great Neck, New York 1

Sundstrand Aviation-Denver
2480 West 70th Avenue
Denver 21, Colorado 1

Mr. James W. Salassi, President
Turbocraft, Inc.
1946 S. Myrtle Avenue
Monrovia, California 1

Universal Match Corporation
Avionics Department Technical Library
4407 Cook Avenue
St. Louis 13, Missouri 1

Waukesha Bearings Corporation
P. O. Box 346
Waukesha, Wisconsin
Attn: Mr. J. M. Gruber, Ch. Engr. 1

Mr. John Boyd
Westinghouse Electric Corporation
Research Laboratories
East Pittsburg, Pennsylvania 1

Mr. H. Walter
Director of Research
Worthington Corporation
Harrison, New Jersey 1

Dr. W. A. Gross
Ampex Corporation
934 Charter Blvd.
Redwood City, California 2

Professor J. Modrey
Department of Mechanical Engineering
Union College
Schenectady 8, New York 2

Stratos Division
Fairchild Stratos Corporation
Bayshore, L. I., New York
Attn: Mr. John Meagher 1

A. C. Spark Plug Division
General Motors Corporation
Route 128
Wakefield, Massachusetts
Attn: Technical Library 1

The Cleveland Graphite Bronze Company
17000 St. Clair Avenue
Cleveland 10, Ohio
Attn: Mr. R. H. Josephson 1

Mr. Richard J. Matt, Manager
Bearing Development & Contract
New Departure Division
General Motors Corporation
Bristol, Connecticut 1

Mr. James J. Barker
10 Walden Avenue
Jericho, New York 1

Thomson Ramo Wooldridge
TAPCO Group
New Devices Laboratories
7209 Platt Avenue
Cleveland 4, Ohio
Attn: Mr. O. Decker 1

Dr. L. Licht
International Business Machines Corp.
Thomas J. Watson Research Center
P. O. Box 218
Yorktown Heights, New York 1

Mr. E. A. Bobley
Union Carbide Nuclear Co.
Post Office Box P
Oak Ridge, Tennessee 1

Lockheed Aircraft Corporation
Missiles and Space Division
Technical Information Center
3251 Hanover Street
Palo Alto, California 1

Office of Technical Services
Department of Commerce
Washington 25, D. C. 1